

DISASTER PREVENTION RESEARCH INSTITUTE

BULLETIN No. 68

MARCH, 1964

ASEISMIC DESIGN METHOD OF ELASTO-
PLASTIC BUILDING STRUCTURES

BY

TAKUJI KOBORI

AND

RYOICHIRO MINAI

KYOTO UNIVERSITY, KYOTO, JAPAN

DISASTER PREVENTION RESEARCH INSTITUTE
KYOTO UNIVERSITY
BULLETIN

Bulletin No. 68

March, 1964

Aseismic Design Method of Elasto-Plastic
Building Structures

By

Takuji KOBORI and Ryoichiro MINAI

Aseismic Design Method of Elasto-Plastic Building Structures

By

Takuji KOBORI and Ryoichiro MINAI

Synopsis

The aseismic design method of an elasto-plastic building structure is discussed. The earthquake response analyses of multi-degree of freedom systems with the bi-linear hysteretic characteristics are carried out by using a digital or analog computer, and the various response diagrams are shown. Particularly, the effects of both the wave shape functions of earthquake excitations and the rigidity ratios of the second bi-linear branches to the first branches on the earthquake responses are taken into consideration. The aseismic design data for the initial structural design are deduced from the optimum dynamic characteristics which make the aseismic safety of a structure be uniform within the prescribed allowable value, and the data are presented here to be available to the practical aseismic design.

Nomenclature

- T, τ ; time and non-dimensional time.
 Y_j ; displacement of the j -th mass with respect to fixed coordinates.
 \bar{Y} ; ground displacement.
 η_j ; non-dimensional displacement of the j -th mass with respect to moving coordinates.
 $\{M_j\}$; mass.
 $\{K_{1j}\}$; rigidity of the first bi-linear branch.
 $\{K_{2j}\}$; rigidity of the second bi-linear branch.
 $\{A_j\}$; relative displacement at elastic limit.
 $\{B_j\}$; strength at elastic limit.
 $\{E_j\}$; potential energy at elastic limit.
 $\{P_j\}$; allowable elasto-plastic potential energy.
 $\{m_j\}, \{\kappa_j\}, \{\delta_j\}, \{\beta_j\}, \{e_j\}, \{p_j\}$; distribution vectors corresponding to $\{M_j\}, \{K_{1j}\}, \{A_j\}, \{B_j\}, \{E_j\}$ and $\{P_j\}$, respectively.

- $\{\gamma_j\}$; rigidity ratio defined by $\{K_{2j}/K_{1j}\}$.
- $\bar{M}, \bar{K}, \bar{A}, \bar{B}, \bar{E}, \bar{P}$; standard values with respect to $\{M_j\}, \{K_{1j}\}, \{A_j\}, \{B_j\}, \{E_j\}$ and $\{P_j\}$.
- $r, \{\mu_j\}$; standard value and distribution vector with respect to $\{\gamma_j\}$.
- $\{\emptyset_j\}$; bi-linear hysteretic characteristics.
- $\varphi_j, \varphi_j^p, \varphi^e$; bi-linear hysteretic characteristic function, perfectly elasto-plastic characteristic function and elastic characteristic function.
- U_i, u_i ; sum of absolute plastic flow with respect to \emptyset_j and corresponding dimensionless value.
- A ; maximum amplitude of ground acceleration.
- $a(T), a(\tau)$; wave shape function of ground acceleration and non-dimensional wave shape function.
- $\alpha, v(=\alpha \cdot \rho)$; non-dimensional intensity parameter with respect to dimensionless ground acceleration and velocity, respectively.
- ρ^{-1} ; non-dimensional frequency parameter of dimensionless earthquake excitation.
- T_a, τ_a ; time constant and non-dimensional time constant (time duration of earthquake excitation and dimensionless time duration).
- $A(T_a)$; frequency characteristics of the maximum amplitude of ground acceleration.
- $C_{\hat{a}}, C_{\hat{v}}, C_{\hat{d}}$; constants corresponding to the constant maximum acceleration, velocity and displacement, respectively.
- T_{au}, T_{al} ; ρ_l^{-1}, ρ_u^{-1} ; upper and lower limits of the time constant in the constant maximum velocity characteristics and those of the non-dimensional frequency parameter.
- ${}_1T, {}_1\tau$; fundamental natural period and non-dimensional fundamental period.
- $\gamma_D = \{\gamma_{dj}\}$; maximum ductility factor.
- $\gamma_E = \{\gamma_{ej}\}$; total dissipated hysteretic energy factor.
- $\gamma_F = \{\gamma_{fj}\}$; offset factor.
- $\{\gamma_{mj}\}$; maximum moment factor.
- $\gamma_M = \gamma_{m1}$; maximum overturning moment factor.
- $\bar{L}, \{l_j\}$; standard value and distribution vector with respect to the height of interstory.
- p ; slope parameter of linear rigidity distribution in the first bi-linear branch.
- c ; index which characterizes the interrelations among distribution vectors,

- corresponding to the type of structural system.
- $\gamma_a, \{\nu_j\}$; standard value and distribution vector with respect to allowable ductility factor $\{\gamma_{allow, j}\}$.
- $\sup_j\{\gamma_{aj}/\nu_j\}, \sup_j\{\gamma_{ej}/\nu_j\}$; maximum values with respect to j of the standardized maximum ductility factor $\{\gamma_{aj}/\nu_j\}$ and the standardized total dissipated hysteretic energy factor $\{\gamma_{ej}/\nu_j\}$, respectively.
- γ_D^m, γ_D^s ; mean and standard deviation with respect to j of the standardized maximum ductility factor $\{\gamma_{aj}/\nu_j\}$.
- $\{\gamma_{aj}^a\}$; deviation of $\{\gamma_{aj}/\nu_j\}$.
- $\{n\tilde{\gamma}_{aj}\}$; normalized random variable corresponding to $\{\gamma_{aj}/\nu_j\}$.
- a, b ; absolute maximum and minimum values of $n\tilde{\gamma}_{aj}$ with respect to j .
- $\tilde{\gamma}_{aj}/\nu_j, \tilde{\gamma}_D^m, \tilde{\gamma}_D^s, \tilde{\gamma}_{aj}^a, \tilde{a}, \tilde{b}$; maximum values with respect to a excitation group.
- $\tilde{\gamma}_e$; $\sup_j\{\gamma_{ej}/\nu_j\}$ due to the most destructive element of a excitation group that produces $\sup_j\{\gamma_{aj}/\nu_j\} = \gamma_a$.
- \tilde{m} ; equivalent cycle number of hysteresis of $\tilde{\gamma}_e$ referred to the hysteretic energy of the loop having a dimensionless amplitude γ_a .
- M_T ; total mass.
- $\{W_j\}, \bar{W}, W_T$; weight, standard value of $\{W_j\}$ and total weight.
- g ; acceleration of gravity.
- E_T, P_T ; total potential energy at elastic limit and total allowable elasto-plastic potential energy.
- $s = \bar{E}/W_T$; base shear coefficient.
- $e_e = \bar{E}/\bar{W}$; elastic potential energy factor.
- $p_e = E_T/W_T$; total elastic potential energy coefficient.
- $e_{ev} = \bar{P}/\bar{W}$; allowable elasto-plastic potential energy factor.
- $p_{ev} = P_T/W_T$; total allowable elasto-plastic potential energy coefficient.
- $\{V_{e^*}\}, \{v_{ej}\}, \bar{V}_e$; equivalent relative velocity for the potential energy at elastic limit, distribution vector and standard value.
- $\{V_{evj}\}, \{v_{evj}\}, \bar{V}_{ev}$; equivalent relative velocity for allowable elasto-plastic potential energy, distribution vector and standard value.
- n, N ; number of degrees of freedom of a structural model and total number of story of a structure.
- $\{M_j\}_N, \{K_{ij}\}_N, \{A_j\}_N, \{B_j\}_N, \{E_j\}_N, \{P_j\}_N$; optimum dynamic characteristics of a structure with the total number of story N .
- $\{m_j\}_N, \{\kappa_j\}_N, \{\delta_j\}_N, \{\beta_j\}_N, \{e_j\}_N, \{p_j\}_N$; optimum distributions of dyna-

- mic characteristics of a structure.
- $\bar{M}_N, \bar{K}_N, \bar{A}_N, \bar{B}_N, \bar{E}_N, \bar{P}_N$; optimum standard values of dynamic characteristics of a structure.
- $\{\kappa_{0j}\}_N, \{\delta_{0j}\}_N, \{\beta_{0j}\}_N, \{e_{0j}\}_N, \{p_{0j}\}_N$; optimum distribution vectors for the case $\{m_j\}_N = \{1\}$.
- $m(x), \kappa(x), \delta(x), \beta(x), e(x), p(x)$; optimum distribution functions for the limiting case $N \rightarrow \infty$.
- $\kappa_0(x), \delta_0(x), \beta_0(x), e_0(x), p_0(x)$; optimum distribution functions for the case $m(x) = 1$.
- $\mu(x), \nu(x)$; distribution functions of rigidity ratio and allowable maximum ductility factor for the limiting case $N \rightarrow \infty$.
- x ; height measured from the ground level.
- H ; total height of structure.
- D ; width of structure in a direction parallel to the applied excitation.
- x_j ; height of the j -th story from the ground level.
- $\{s_j\}_N$; shear coefficient.
- $\{s_j/s\}_N$; distribution vector of shear coefficient.
- $\{f_j\}_N, f(x)$; modifying coefficient and function for the non-uniform mass distribution.
- $\{k_j\}_N, k(x)$; lateral force coefficient.
- $\{k_j/s\}_N, k(x)/s$; distribution vector and function of lateral force coefficient referred to the base shear coefficient.
- $\{k_{0j}/s\}_N, k_0(x)/s$; distribution vector and function of lateral force coefficient for the case $\{m_j\}_N = \{1\}$ and $m(x) = 1$, respectively.
- $\{F_j\}_N$; lateral force.
- ${}_1\tau_N$; non-dimensional fundamental period of the N -degree of freedom system.
- \bar{W}_N ; standard value of weight of the structure with the total number N of story.
- $\{V_{evj}\}_N, \{v_{evj}\}_N, \bar{V}_{evN}$; equivalent relative velocity, distribution vector and standard value of the structure with the total number N of story.
- θ_e ; equivalent rotational angle of interstory at elastic limit.
- ${}_1T_l, {}_1T_u$; upper and lower limits of fundamental natural period in the domain characterized by the constant maximum velocity.
- d_i, d, e ; constants referred to the base shear coefficient.

A_E, A_R ; safety factors corresponding to a earthquake excitation group and the measure of aseismic safety.

$\delta_T(x)$; delta-function.

$A_I(=A_{II}), B_I, B_{II}, C_I, C_{II}$; classification of dynamic characteristics.

$A : p=0, \quad B : p=3/2, \quad C : p=3.$

$I : c=1, \quad II : c=1/2.$

1. Introduction

The aseismic design of a building structure should be intended to assign the reasonable dynamic characteristics to the structure so that the earthquake responses to a group of the prescribed earthquake excitations remain uniformly within their allowable values. The principle and the method of the aseismic design are not to be uniquely determined, since they should be appropriately chosen depending on the structural materials, the type of the structural system, the function of the building, the frequency of occurrence and the intensity of earthquake excitations, the mechanism of earthquake shocks and so on. A typical structural frame composed of ductile materials should be designed in accordance with the following two methods depending upon the nature of earthquakes. The ultimate elasto-plastic aseismic design method should be applied to the case of very intense earthquakes with small frequency of occurrence. On the other hand, the elastic aseismic design method, either statistical or non-statistical, should be considered to the case of moderately intense earthquakes with large frequency of occurrence^{1~4)}. To establish the suitable design method corresponding to the specific principle of the aseismic design, the following two stages should be considered. At the first stage, the aseismic design data for the members and joints of a structure should be reasonably obtained by earthquake response analyses; namely, a group of earthquake excitations, a model of structural system and the various measures of aseismic safety should be comprehensively considered. Then the optimum dynamic characteristics of the structural system can be determined by parametric survey. These optimum dynamic characteristics determined only from the standpoint of earthquake engineering must be different from the dynamic characteristics of the real structure designed under the actual load conditions. And the real aseismic safety of a structure may not always be guaranteed by the comprehensive estimation

of the aseismic safety at this first stage. Therefore, at the second stage, the concrete and strict model of a structural system is chosen and the aseismic safety should be reexamined in details by the full measures with respect to each structural element^{5,6)}.

In this paper, we will discuss only about the first stage of the ultimate elasto-plastic aseismic design method for the ductile structural frames, and will present the procedure to obtain the design data which are the base shear coefficient, the distribution of lateral force coefficients and so on.

2. Basic procedure of ultimate elasto-plastic aseismic design method at the first stage

Comprehensively to obtain the aseismic design data at the first stage, all variable quantities and parameters are desirable to be dimensionless in the earthquake response analyses. The aseismic design data can be obtained by the following procedure.

a) **The supposition of a group of earthquake excitations:** Any earthquake excitation can be expressed by the product of the wave shape function with a time constant and the maximum amplitude of acceleration. And the excitation group can be defined by the frequency characteristics of the maximum acceleration amplitude. Here, as the typical patterns of acceleration excitation, we pick up two different non-dimensional wave shape functions which are normalized so that the mean is zero and the

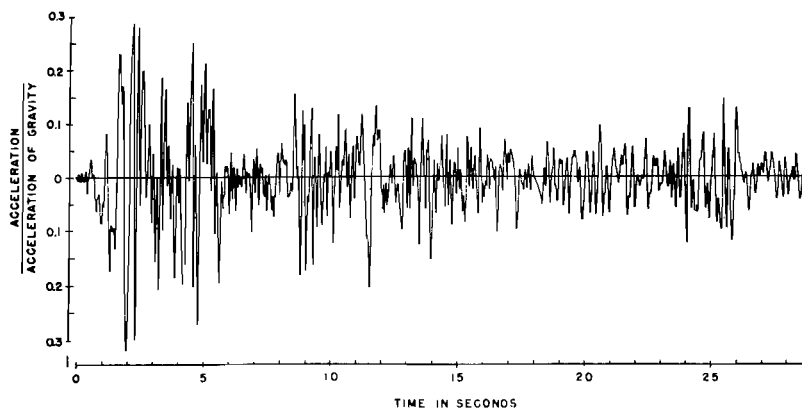


Fig. 1. (a) Accelerogram for El Centro, California, May 18, 1940, N-S Component.

maximum value is unity ; those of El Centro, California, May 18, 1940, earthquake N-S component and Vernon, California, Oct. 2, 1933, earthquake S82°E component. The former seems to be almost a random stationary function and to have a large power ratio defined as the power ratio of a random component to the predominant periodic components as shown in Figs. 1~3. The latter seems to be a non-stationary random function and to have a comparatively small power ratio as shown in Figs. 4~6⁷⁾. The

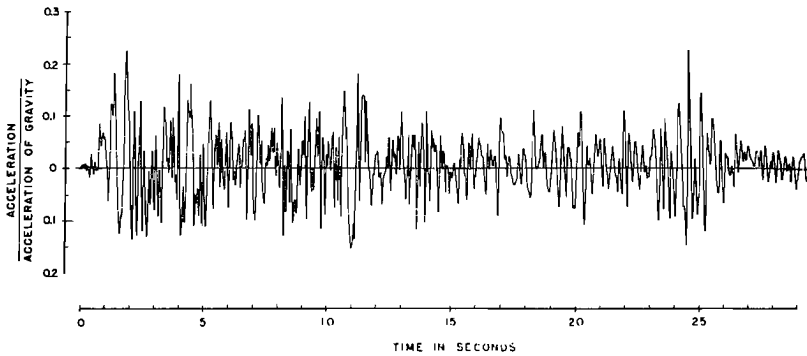


Fig. 1. (b) Accelerogram for El Centro, California, May 18, 1940, E-W Component.

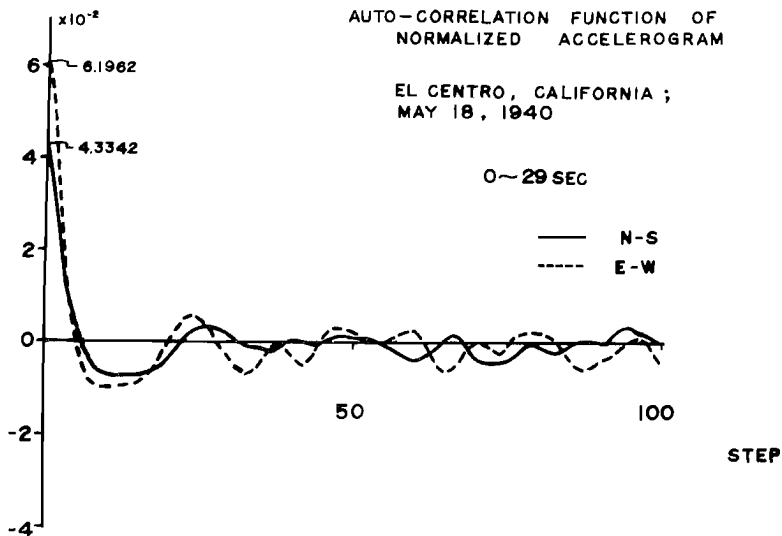


Fig. 2. Autocorrelation Functions of Normalized Accelerograms of El Centro Earthquake.

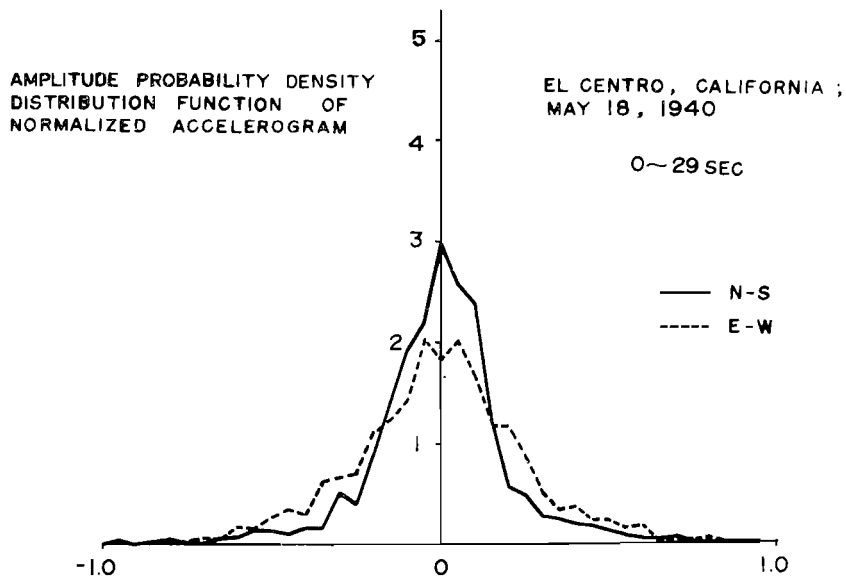


Fig. 3. Amplitude Probability Density Distribution Functions of Normalized Accelerograms of El Centro Earthquake.

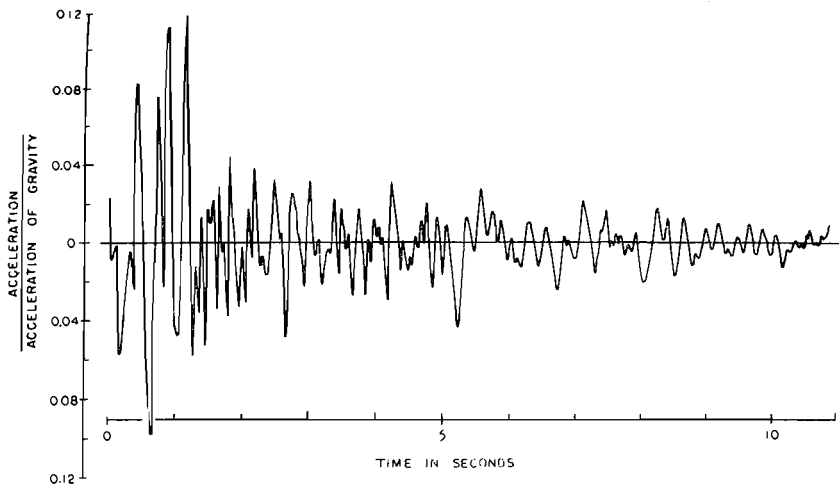


Fig. 4. (a) Accelerogram for Vernon, California, Oct. 2, 1933, S82°E Component.

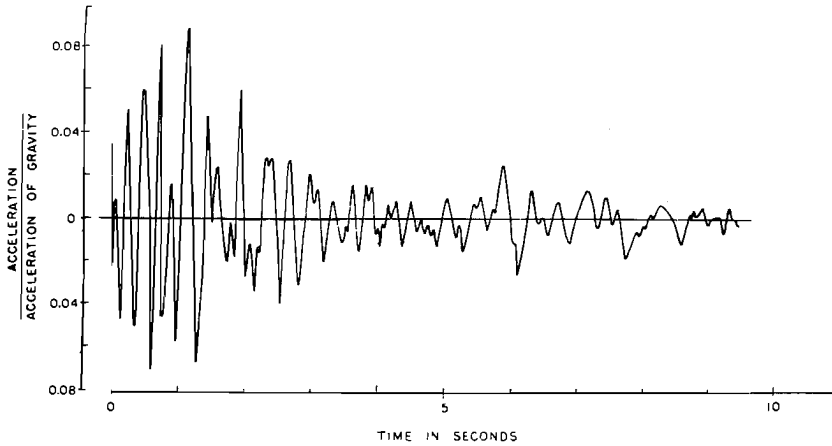


Fig. 4. (b) Accelerogram for Vernon, California, Oct. 2, 1933, N08°E Component.

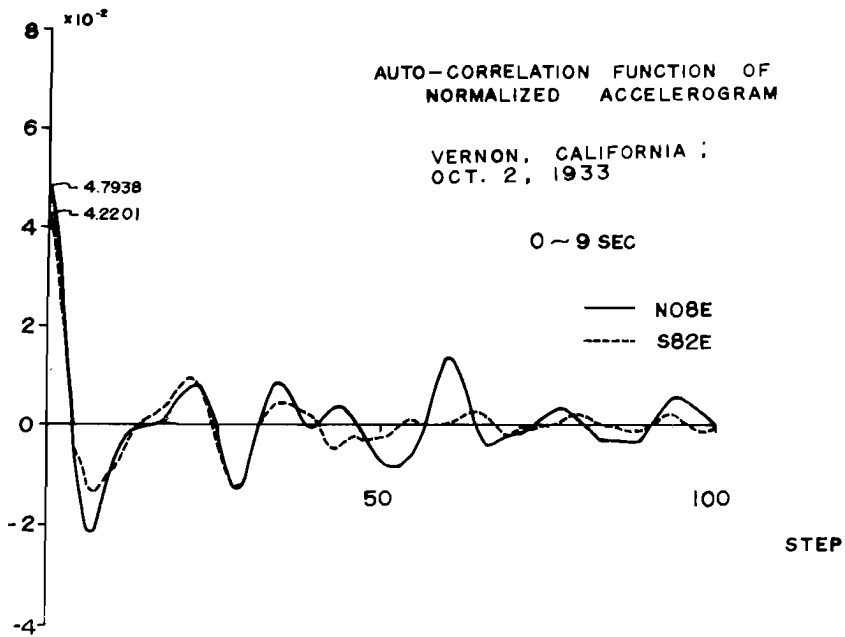


Fig. 5. (a) Autocorrelation Functions of Normalized Accelerograms of Vernon Earthquake, 0~9 sec.

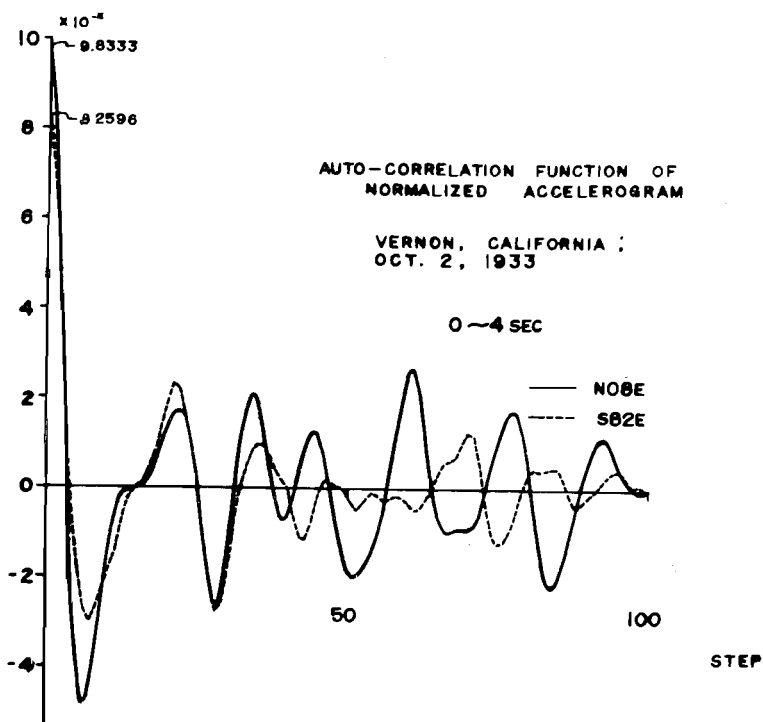


Fig. 5. (b) Autocorrelation Functions of Normalized Accelerograms of Vernon Earthquake, 0~4 sec.

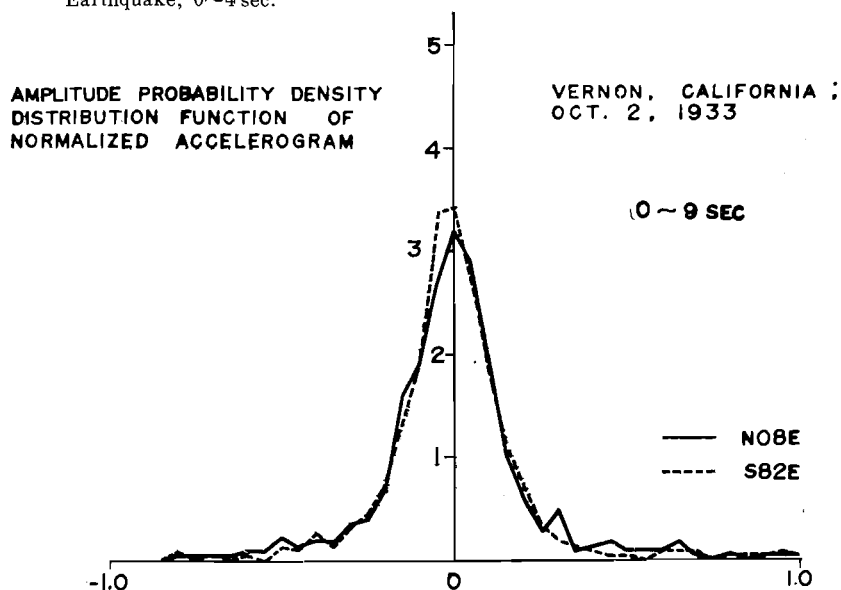


Fig. 6. (a) Amplitude Probability Density Distribution Functions of Vernon Earthquake, 0~9 sec.

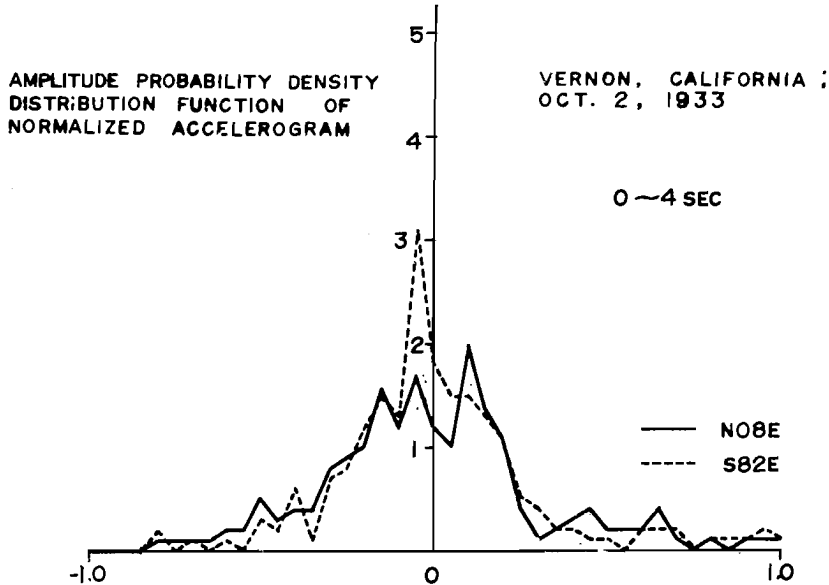


Fig. 6. (b) Amplitude Probability Density Distribution Functions of Vernon Earthquake, 0~4 sec.

frequency characteristics of the maximum acceleration amplitude are assumed to be the constant maximum acceleration in the high frequency range, the constant maximum velocity in the intermediate frequency range, and the constant maximum displacement in the low frequency range, respectively. The constants contained in the frequency characteristics may be appropriately chosen so that the maximum quantities of the excitation group are reasonable to the very intense earthquake excitations, under consideration of the safety factor A_E , referring to the typical ground motion records of the earthquakes. Here, we determine the frequency characteristics of the two excitation groups of El Centro and Vernon earthquakes under the assumption that the maximum of the maximum acceleration amplitudes is $0.4g$ and the maxima of the maximum velocity amplitudes and of the maximum displacement amplitudes are in the ranges from 35 to 40 cm/sec and from 40 to 50 cm, respectively.

b) The supposition of the model of a structural system : The dynamic characteristics are expressed by a set of the products of the distributions and the corresponding standard values of the physical quantities of the structural system. The non-dimensional dynamic model defined as a set

of the distributions should be comprehensive and essential as well as concrete and realistic, though the supposition of the model is nothing but the restriction to the structural system to be design. And also, it should be noticed that the model must contain the dimensionless design parameters which have primarily important effects on the earthquake responses. Thus the model is supposed to be a multi-degree-of-freedom shear type system with the bi-linear hysteretic characteristics. And all effects of the viscous damping, bending and torsional vibrations, and the ground-structure coupling vibration are neglected here^{2,5,8)}. Then the dynamic characteristics of the non-dimensional model consist of the distribution vectors and the rigidity ratios of the second bi-linear branches to the first branches. The distribution vectors are concerned to mass, rigidity of the first bi-linear branch, and strength or relative displacement or elastic potential energy at the elastic limit. And the rigidity ratios can be expressed as the product of a distribution vector and a standard value.

c) The selection of the measures of aseismic safety and the estimation of earthquake responses : The earthquake responses and their allowable responses should be estimated in terms of the measures of aseismic safety. The ductility factor⁹⁾ which concerns to the instantaneous deformation, as an important measure of the comprehensive aseismic safety, and the dissipated hysteretic energy factor related to the cyclic fatigue, as another important measure, are introduced here. Namely, the former is defined as the ratio of the elasto-plastic relative displacement to the relative displacement at the elastic limit, and the latter as the ratio of the dissipated hysteretic energy to the potential energy at the elastic limit, respectively. Then the basic responses of the structural model can be defined as the maximum ductility factor and the total dissipated hysteretic energy factor with respect to time. And so the aseismic safety can be estimated by comparing these quantities with the corresponding allowable values obtained from the ultimate values over the proper safety factor A_R . Also as auxiliary responses, the offset factor and the overturning moment factor are introduced here. The former means the ratio of the permanent set with respect to the relative displacement to the elastic limit and the latter the ratio of the overturning moment due to a earthquake excitation to the elastic resisting moment.

d) Non-dimensional earthquake response analysis and the basic re-

sponse diagram : To determine the optimum dynamic characteristics, the non-dimensional earthquake responses should be analyzed with respect to the various sets of distributions of the dynamic characteristics and the appropriate non-dimensional wave shape functions of earthquake excitations. And they should be calculated in the wide domain of independent parameters of non-dimensional earthquake, which are defined by the physical quantities of the structural system and the earthquake excitations. Thus these numerical results are expressed as the basic response and auxiliary response diagrams for the specific distributions of the dynamic characteristics and the non-dimensional wave shape function.

e) The determination of the optimum dynamic characteristics : The optimum dynamic characteristics¹¹⁾ are to be determined to control the maximum earthquake responses of the structural system uniformly within their allowable values for a group of prescribed earthquake excitations. This can be done from the basic response diagrams considering the allowable values of responses, the fundamental natural period of the structural system and the frequency characteristics of the maximum acceleration amplitude, if the type of the structural system is prescribed. Here it is convenient to separate the optimum dynamic characteristics into two sets of optimum distributions and corresponding standard values.

i) The determination of the distributions of the optimum dynamic characteristics : The distributions of the optimum dynamic characteristics should be measured by the ratio of the mean to the standard deviation with respect to the basic responses divided by the corresponding distribution coefficients of the allowable values of the responses in the sense that these distributions make the aseismic safety to be uniform. These optimum distributions can be determined so as to make the above-mentioned measure to be large as possible in the appropriately wide domain of the independent parameters of the non-dimensional earthquake.

ii) The determination of the standard values of the optimum dynamic characteristics : The optimum standard values can be obtained from the basic response diagram with respect to the optimum distributions under the condition that the earthquake responses remain within the corresponding allowable values, that is, the maximum of the basic responses over the corresponding distribution coefficients of allowable values is not to be greater than the standard value of allowable values.

The above-obtained optimum dynamic characteristics can be easily applied to the real structural system with multiple degrees of freedom.

f) The determination of aseismic design data at the first stage :

The aseismic design data which mean the several distribution data with respect to the lateral force coefficients, the shear coefficients and the allowable elasto-plastic potential energy etc. can be easily introduced from the optimum distributions. While the base shear coefficient, the allowable elasto-plastic potential energy factor, the total allowable elasto-plastic potential energy coefficient and the formulas to calculate the natural periods of the structural system etc. can be easily deduced as the functions of known or presumable design parameters from the standard values of the optimum dynamic characteristics.

In the following sections, we divide them into three subsections. In the first subsections (3.1, 4.1, 5.1), we study on the basic equations under the above-mentioned assumptions. In the second subsections (3.2, 4.2, 5.2), we discuss about the earthquake response problem of the ductile structure assuming a three degrees of freedom system with perfectly elasto-plastic characteristics and the El Centro type wave shape function. And in the third subsections (3.3, 4.3, 5.3), we consider mainly on the tall, ductile structure of the bi-linear elasto-plastic characteristics under the supposition of a five degrees of freedom system and two typical different wave shape functions (i.e., El Centro type and Vernon type), to clarify the effects of the slightly positive rigidities of the second bi-linear branches and the wave shape function on the earthquake responses and aseismic design data^{2, 10, 12)}.

3. Earthquake response analyses and response diagrams

3.1 According to the suppositions concerning the group of earthquake excitations and the model of structural system, the non-dimensional fundamental differential equation for the earthquake response analysis can be expressed by

$$m_j \frac{d^2 \eta_j}{d\tau^2} + \kappa_j \varphi_j(\eta_j - \eta_{j-1}; \gamma_j, \delta_j) - \kappa_{j+1} \varphi_{j+1}(\eta_{j+1} - \eta_j; \gamma_{j+1}, \delta_{j+1}) = -m_j \alpha \cdot a(\tau) \quad (1)$$

$$j = 1, 2, \dots, n, \quad \eta_0 = 0, \quad \eta_n = \eta_{n+1}$$

where

$$\tau = \sqrt{\bar{K}/\bar{M}} \cdot T, \quad \eta_j = (Y_j - \bar{Y})/\bar{\Delta}, \quad (2)$$

$$\left. \begin{aligned} m_j &= M_j/\bar{M}, \quad \kappa_j = K_{1j}/\bar{K}, \quad r_j = K_{2j}/K_{1j}, \quad \delta_j = \Delta_j/\bar{\Delta}, \\ \beta_j &= \kappa_j \delta_j = B_j/\bar{B} = K_{1j} \Delta_j / \bar{K} \bar{\Delta}, \\ \varphi_j(\eta_j - \eta_{j-1}; r_j, \delta_j) &= \Phi_j(Y_j - Y_{j-1}; K_{1j}, K_{2j}, \Delta_j) / K_{1j} \bar{\Delta} \end{aligned} \right\} (3)$$

$$\alpha = A \bar{M}/\bar{B} = A \bar{M}/\bar{K} \bar{\Delta}, \quad \alpha(\tau) = a(\sqrt{\bar{M}/\bar{K}} \cdot \tau) = (d^2/dT^2) \bar{Y}/A|_{T=\sqrt{\bar{M}/\bar{K}} \cdot \tau}$$

$$\rho = \tau \alpha / {}_1T = T_a / {}_1T \quad (4)$$

And the group of earthquake excitations is to be given by the following frequency characteristics of the maximum acceleration amplitude A .

$$\frac{d^2 \bar{Y}}{dT^2} = A \cdot a(T), \quad A = A(T_a) \quad (5)$$

$$\begin{aligned} A &= C_{\hat{a}}, \quad T_a < T_a \quad && : \text{constant maximum acceleration} \\ A &= C_{\hat{v}} T_a^{-1}, \quad T_{au} \leq T_a \leq T_{al} \quad && : \text{constant maximum velocity} \\ A &= C_{\hat{d}} T_a^{-2}, \quad T_{au} < T_a \quad && : \text{constant maximum displacement} \end{aligned} \quad (6-a)$$

where T : time, Y_j : displacement of the j -th story with respect to the fixed coordinate, M_j : mass of the j -th story, Φ_j : bi-linear hysteretic characteristic of the j -th story, K_{1j} , K_{2j} : each rigidity of the first and second bi-linear branch of Φ_j , Δ_j , B_j : relative displacement and strength at the elastic limit of Φ_j , \bar{M} , \bar{K} , $\bar{\Delta}$, \bar{B} : standard values of mass, rigidity, displacement and strength, n : number of degrees of freedom or total number of stories of the model, $\bar{Y} = Y_0$: ground displacement, A : maximum amplitude of ground acceleration, $a(T)$: wave shape function of ground acceleration, T_a : time constant (time duration), ${}_1T$: fundamental natural period, $C_{\hat{a}}$, $C_{\hat{v}}$, $C_{\hat{d}}$: constants corresponding to the constant maximum acceleration, velocity and displacement, respectively, T_{au} , T_{al} : upper and lower limit of time constant T_a in the range of the constant maximum velocity.

$a(T)$ is the normalized wave shape function of the accelerogram of the El centro or the Vernon earthquake. T_a is the time duration of an earthquake excitation and has a concept of time constant which corresponds uniquely to the peak frequency of the spectral density of $a(T)$. Such a supposition of a group of earthquake excitations may be necessary to obtain the stable structural design for the essentially indeterminable and unpredictable violent earthquakes. For the very intense earthquake excitation groups, the constants $C_{\hat{a}}$, $C_{\hat{v}}$, $C_{\hat{d}}$, T_{al} and T_{au} are chosen here as follows

$$\begin{aligned} \text{El Centro type : } C_{\hat{a}} &= 0.4g = 3.92 \times 10^2 \text{ cm/sec}^2, \quad C_{\hat{v}} = 10^4 \text{ cm/sec}, \\ C_{\hat{d}} &= 7.65 \times 10^6 \text{ cm} \\ T_{a1} &= 25.5 \text{ sec}, \quad T_{au} = 76.5 \text{ sec} \end{aligned} \quad (6-b)$$

$$\begin{aligned} \text{Vernon type : } C_{\hat{a}} &= 0.4g = 3.92 \times 10^2 \text{ cm/sec}^2, \quad C_{\hat{v}} = 4.30 \times 10^8 \text{ cm/sec}, \\ C_{\hat{d}} &= 1.42 \times 10^8 \text{ cm} \\ T_{a1} &= 11.0 \text{ sec}, \quad T_{au} = 33.0 \text{ sec} \end{aligned} \quad (6-c)$$

The frequency characteristics defined by eq. (6-a) can be expressed by the following equation, using the non-dimensional intensity and frequency parameters α and ρ^{-1} defined by eq. (4) which are two independent parameters of a non-dimensional acceleration excitation.

$$\left. \begin{aligned} \alpha &= C_{\hat{a}} \bar{M} / \bar{B}, \quad \rho < \rho_l = T_{a1} / T \\ \alpha \rho &= C_{\hat{v}} \sqrt{\bar{M} \bar{K}} / {}_1\tau \bar{B}, \quad \rho_l \leq \rho \leq \rho_u = T_{au} / T \\ \alpha \rho^2 &= C_{\hat{d}} \bar{K} / {}_1\tau^2 \bar{B}, \quad \rho_u < \rho, \quad {}_1\tau = {}_1\tau(\{m_j\}, \{\kappa_j\}) \end{aligned} \right\} \quad (7)$$

where ${}_1\tau$ is the non-dimensional fundamental period determined only from the distribution vectors $\{m_j\}$ and $\{\kappa_j\}$ in the elastic range. If we choose v instead of α , the intensity parameter v becomes

$$v = \alpha \rho = \frac{AT_a}{(\bar{B}/\bar{M})_1 T} = \frac{AT_a}{\sqrt{2} {}_1\tau \sqrt{\bar{E}/\bar{M}}}, \quad \bar{E} = \frac{\bar{B}\bar{d}}{2} \quad (8)$$

This is proportional to the maximum velocity amplitude of earthquake excitation and to the reciprocal of the root of elastic limit potential energy per unit mass. And so the frequency characteristics expressed by eq. (7) becomes

$$\left. \begin{aligned} v \rho^{-1} &= C_{\hat{a}} \bar{M} / \bar{B}, \quad \rho < \rho_l \\ v &= C_{\hat{v}} \sqrt{\bar{M} \bar{K}} / {}_1\tau \bar{B}, \quad \rho_l \leq \rho \leq \rho_u \\ v \rho &= C_{\hat{d}} \bar{K} / {}_1\tau^2 \bar{B}, \quad \rho_u < \rho \end{aligned} \right\} \quad (9)$$

The maximum ductility factor γ_D and the total dissipated hysteretic energy factor γ_E to be considered as the basic responses are expressed by the following relations, respectively.

$$\gamma_D = \{\gamma_{a_j}\} = \{|\eta_j - \eta_{j-1}|_{max} / \delta_j\} = \{ |Y_j - Y_{j-1}|_{max} / d_j \} \quad (10)$$

$$\gamma_E = \{\gamma_{e_j}\} = \{2u_j / \delta_j\} = \{2U_j / d_j\} \quad (11)$$

where U_j is the sum of the absolute values of plastic deformations of the j -th story.

The bi-linear hysteretic characteristic function φ_j is to be expressed by the sum of two terms.

$$\begin{aligned}\varphi_j(\eta_j - \eta_{j-1}; r_j, \delta_j) &= (1 - r_j) [\varphi_j^p + (r_j / (1 - r_j)) \varphi_j^e] \\ \varphi_j^p &= \varphi_j(\eta_j - \eta_{j-1}; 0, \delta_j), \quad \varphi_j^e = \varphi_j(\eta_j - \eta_{j-1}; 1, \infty)\end{aligned}\quad (12)$$

In eq. (12), φ_j^p represents the perfectly elasto-plastic characteristic function and φ_j^e the elastic characteristic function, respectively. Therefore, the hysteretic dissipated energy is contributed by the first term. Then the total dissipated hysteretic energy factor γ_E can be expressed in the form of eq. (11).

$$\gamma_{Ej} = 2K_{1j}(1 - r_j) \Delta_j U_j / K_{1j}(1 - r_j) \Delta_j^2 = 2U_j / \Delta_j \quad (13)$$

The offset factor γ_E and the maximum moment factor $\{\gamma_{mj}\}$ introduced as auxiliary responses are expressed by the following relations, respectively.

$$\begin{aligned}\gamma_E &= \{\gamma_{rj}\} = \left\{ (1 - r_j) \left[\frac{(\eta_j - \eta_{j-1})r}{\delta_j} - \text{sgn } \varphi_j((\eta_j - \eta_{j-1})r; r_j, \delta_j) \right] \right\} \\ &= \left\{ (1 - r_j) \left[\frac{(Y_j - Y_{j-1})r}{\Delta_j} - \text{sgn } \Phi_j((Y_j - Y_{j-1})r; K_{1j}, K_{2j}, \Delta_j) \right] \right\}\end{aligned}\quad (14\text{-a})$$

$$\{\gamma_{mj}\} = \left\{ \frac{\left| \sum_{i=j+1}^n l_i \kappa_i \varphi_i + \left(\sum_{i=1}^j l_i \right) \kappa_j \varphi_j \right|_{max}}{\beta_j l_j} \right\} = \left\{ \frac{\left| \sum_{i=j+1}^n L_i \Phi_i + \left(\sum_{i=1}^j L_i \right) \Phi_j \right|_{max}}{B_j L_j} \right\} \quad (14\text{-b})$$

And the maximum overturning moment factor γ_M is defined by the maximum moment factor of the first story. Thus γ_M means the ratio of the maximum absolute value of the overturning moment at the basement to the standard value of the elastic resisting moment.

$$\gamma_M = \gamma_{m1} B_1 L_1 / \bar{B} \bar{L} = \left| \sum_{i=1}^n l_i \kappa_i \varphi_i \right|_{max} = \left| \sum_{i=1}^n L_i \Phi_i \right|_{max} / \bar{B} \bar{L} \quad (15)$$

$$\text{where} \quad (\eta_j - \eta_{j-1})_r = (Y_j - Y_{j-1})_r / \bar{\Delta} \quad l_i = L_j / \bar{L} \quad (16)$$

$(Y_j - Y_{j-1})_r$ is the final maximum amplitude of the elastic relative displacement of the j -th story. L_j is the height of the j -th story. And \bar{L} is the standard value of the height of interstory.

As regards the dynamic characteristics of the structural model, the following independent quantities are introduced by

$$\left. \begin{aligned}\{M_j\} &= \bar{M}\{m_j\}, \quad \{\Delta_j\} = \bar{\Delta}\{\delta_j\} \\ \{K_{1j}\} &= \bar{K}\{\kappa_j\}, \quad \{K_{2j}\} = \bar{K}\{r_j \kappa_j\} = \bar{K}r\{\mu_j \kappa_j\}\end{aligned}\right\} \quad (17)$$

where $\{m_j\}$, $\{\kappa_j\}$, $\{\delta_j\}$, $\{\mu_j\}$, are distribution vectors and \bar{M} , \bar{K} , $\bar{\Delta}$, r are the corresponding standard values, respectively. For the convenience of earthquake response analyses, we presuppose that the distribution $\{m_j\}$ of masses and the rigidity ratios $\{r_j\}$ of the second bi-linear branches to the

first branches are uniform and also the rigidity distribution $\{\kappa_j\}$ of the first branches is linear, and that the relation between $\{\kappa_j\}$ and $\{\delta_j\}$ or $\{\beta_j\}$ is characterized by the index c from $1/2$ to 1 , corresponding to the type of structural system. That is to say,

$$\begin{aligned} \{m_j\} &= \{1\}, \quad \{\mu_j\} = \{1\} \\ \{\kappa_j\} &= \left\{ \frac{2n + p[2(n-j) + 1]}{2n + p[2n - 1]} \right\} \\ \{\delta_j\} &= \{\kappa_j^{c-1}\}, \text{ i.e., } \{\beta_j\} = \{\kappa_j^c\}, \quad 1/2 \leq c \leq 1 \\ j &= 1, 2, \dots, n \end{aligned} \quad (18)$$

For the standard values of the dynamic characteristics, the corresponding values of the first story are always selected.

3.2 To find the general characters of the non-dimensional earthquake responses and to obtain the seismic design data of the ductile structural system with an arbitrary fundamental natural period, we will analyze the basic responses under the assumptions that the number n of degrees of freedom of the model is equal to three ($n=3$) and the rigidity ratio parameter r has zero value ($r=0$) and also that the wave shape function is El Centro type. As the two independent parameters of non-dimensional earthquake excitation, α and ρ are chosen, and their domain in which the response analyses have to be mainly done is roughly estimated by considering the relation between the group of earthquake excitations and the structural system to be designed. Particularly the main variable range of ρ can be almost determined only from the property of the wave shape function of the earthquake excitations. This range is also suggested from the results of the previous earthquake response analyses^{9, 12, 13}. Assuming that the structural system has the fundamental natural period ranging from 1 second to 2 seconds and that the base shear coefficient is smaller than 0.3, the domain $0.4 \leq \alpha \leq 1.2$, $15 \leq \rho \leq 50$ can be presupposed. To determine the optimum dynamic characteristics, five sets of distribution vectors are chosen. They are denoted by $A_I = A_{II}$, B_I , B_{II} , C_I and C_{II} , where A , B and C denote respectively their slope p of the linear distribution of rigidity, i.e., $A: \{\kappa_j\} = \{1, 1, 1\}$, $B: \{\kappa_j\} = \{1, 7/9, 5/9\}$, $C: \{\kappa_j\} = \{1, 5/7, 3/7\}$, and the subscripts I and II denote the index c of the structural system defined by the third equation of eq. (18), i.e., $I: c=1$, $II: c=1/2$. The latter classification corresponds to the type of structures. That is to say, I and II represent the idealized braced and the idealized framed

structure, respectively. The ordinary structures may be in between *I* and *II*.

Thus the numerical calculations based on the Runge Kutta's third order procedure are carried out by means of Kyoto University Digital Computer, KDC-I. As the results, some of the basic response diagrams for the maximum ductility factor $\gamma_D = \{\gamma_{aj}\}$ and the total dissipated hysteretic energy factor $\gamma_E = \{\gamma_{ej}\}$ are shown in Figs. 7~12. These basic response diagrams show the similar qualitative trend though the basic response diagrams of γ_E are smoother than those of γ_D . Both of them are the increasing functions of α and ρ , and their values increase abruptly when ρ becomes greater than a specific value. And also they are gradually dispersed with respect to space level j when both values of α and ρ are increased. But it is found that if we choose v instead of α as an intensity parameter, the basic responses become the weak functions of the frequency parameter ρ^{-1} . From the similarity between the two basic responses, it is pointed out that the ductility factor can be regarded as the only basic measure of aseismic safety. This corresponds to the fact that the most of the total dissipated

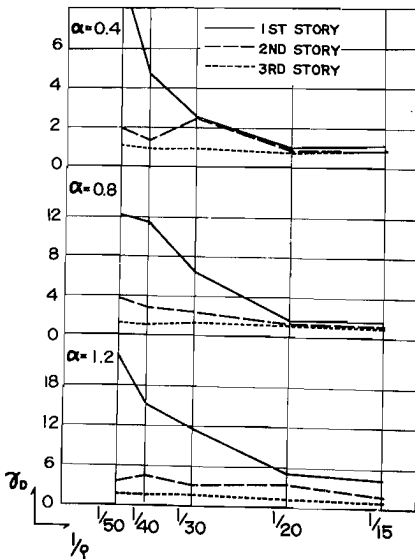


Fig. 7. Basic Response Diagram of Maximum Ductility Factor-El Centro N-S, Structural Model $A_I = A_{II}$.

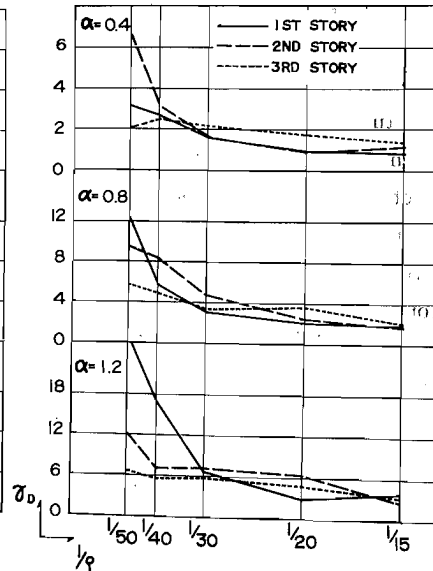


Fig. 8. Basic Response Diagram of Maximum Ductility Factor-El Centro N-S, Structural Model B_I .

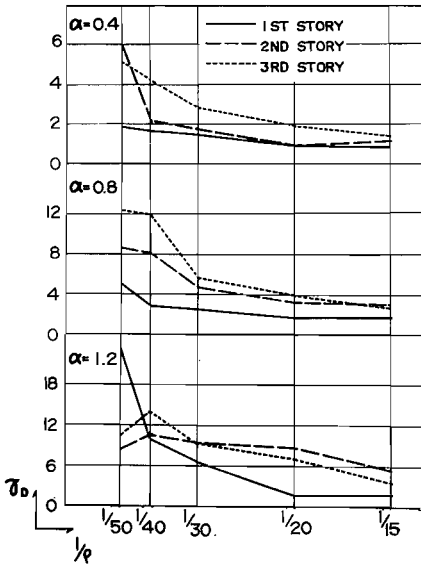


Fig. 9. Basic Response Diagram of Maximum Ductility Factor-El Centro N-S, Structural Model C_I .

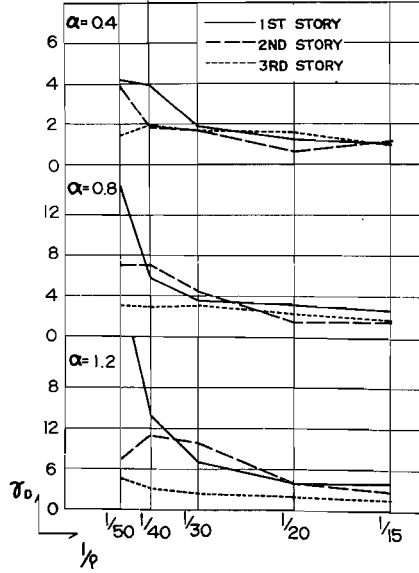


Fig. 10. Basic Response Diagram of Maximum Ductility Factor-El Centro N-S, Structural Model C_{II} .

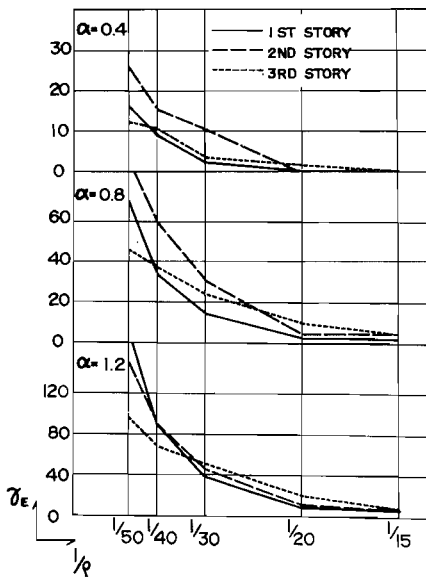


Fig. 11. Basic Response Diagram of Total Dissipated Hysteretic Energy Factor-El Centro N-S, Structural Model B_I .

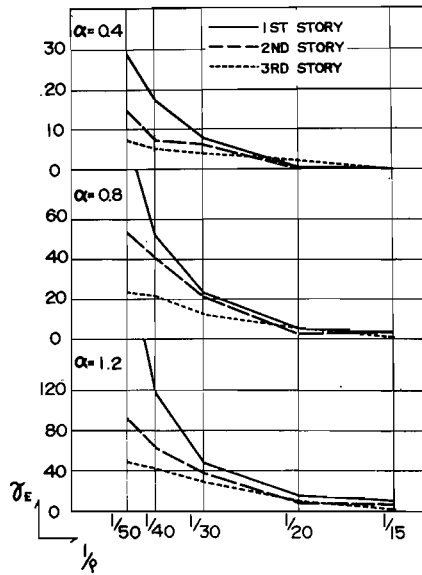


Fig. 12. Basic Response Diagram of Total Dissipated Hysteretic Energy Factor-El Centro N-S, Structural Model C_{II} .

hysteretic energy is contributed to a few cycles of relative displacement with large ductility factor. As both values of α and ρ become larger, the instability of the basic responses may be considerably prevented by the both effects of the slightly positive rigidities of the second branches in the bi-linear hysteretic characteristics and of the internal viscous dampings^{9~12)}.

3.3 Particularly to obtain the aseismic design data of tall, elasto-plastic structural system with the long fundamental natural period from 2 to 5 seconds, the non-dimensional earthquake responses of a five degrees of freedom system are analyzed by an indirect, slow type electronic analog computer in Department of Architecture, Kyoto University. In this case the two typical different non-dimensional wave shape functions of the El Centro and the Vernon type are considered. And the uniformly distributed mass $\{m_j\}=\{1\}$ and rigidity ratios $\{r_j\}=\nu\{1\}$ are introduced here. And also the standard value ν of the rigidity ratios is supposed to be 0, 0.1 and 0.2. Then the maximum ductility factor γ_D , the offset factor γ_F and the maximum overturning moment factor γ_M defined by eqs. (10), (14-a) and (15) are computed in the appropriate domain of the parameters of the non-dimensional earthquakes, provided that the range of the intensity parameter ν defined by eq. (8) is determined so as to produce the responses with the maximum ductility factors γ_{d_j} from 1 to 5, and provided that the range of the frequency parameter ρ^{-1} defined by eq. (4) can be determined from both the fundamental natural period $1T$ of the structure and the frequency characteristics of the earthquake excitation group. For the convenience of analyses the structural model is limited to only two kinds B_I type and C_{II} type, which seem to be suitable in a sense of uniformly distributed aseismic safety. Both B_I and C_{II} type are characterized by the set of two quantities p and c defined by eq. (18); that is, ($p=3/2$, $c=1$) and ($p=3$, $c=1/2$), respectively. The computed results are shown in Figs. 13~21. As a general trend, the earthquake responses γ_D , γ_F and γ_M are all the increasing functions of ν , among which γ_D and γ_M are the weak functions of ρ^{-1} . Clearly the variances of γ_D and γ_F are the increasing functions of ν and the decreasing functions of ν . The effect of ν on γ_D is large particularly in the slightly positive range, and is decreasing gradually when ν is increasing. But, the effect of ν on γ_F is not decreasing so much as that of ν on γ_D , from the following equation.

$$\gamma_{Fj} \cong (1 - r_j) / r_j \quad (19)$$

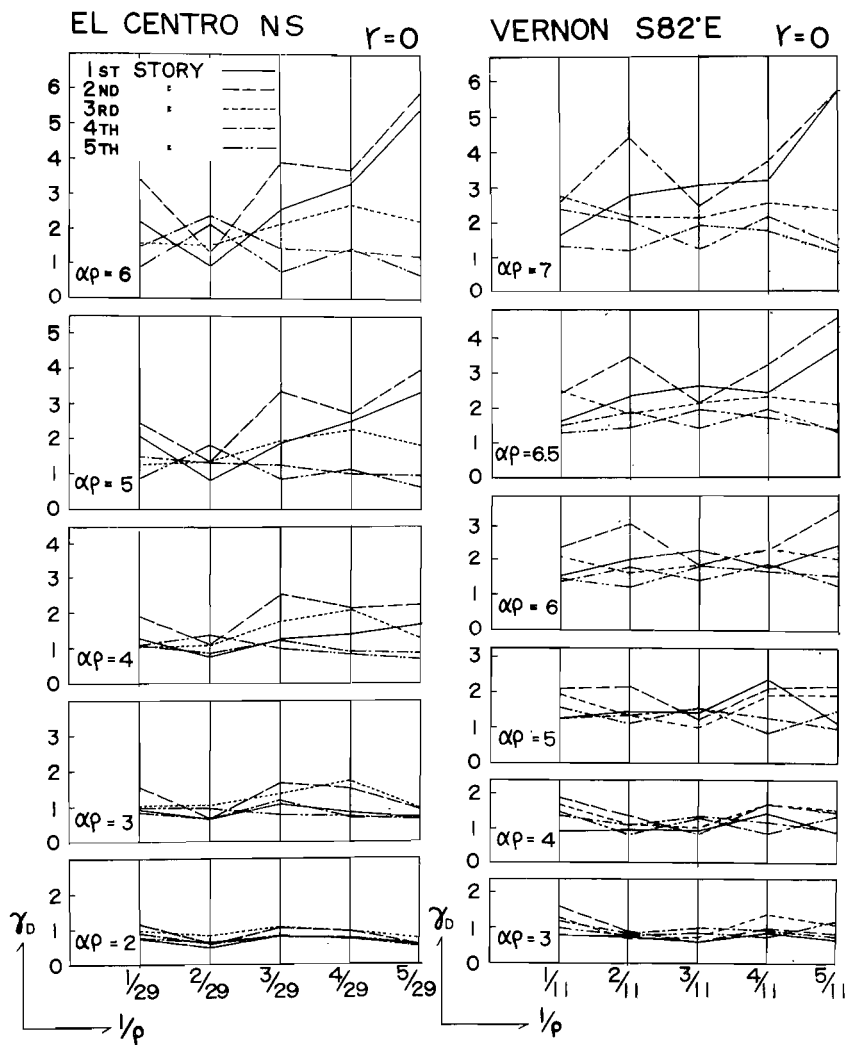


Fig. 13. Basic Response Diagrams of Maximum Ductility Factor-El Centro N-S and Vernon S82°E, Structural Model B_I , Rigidity Ratio $r=0$.

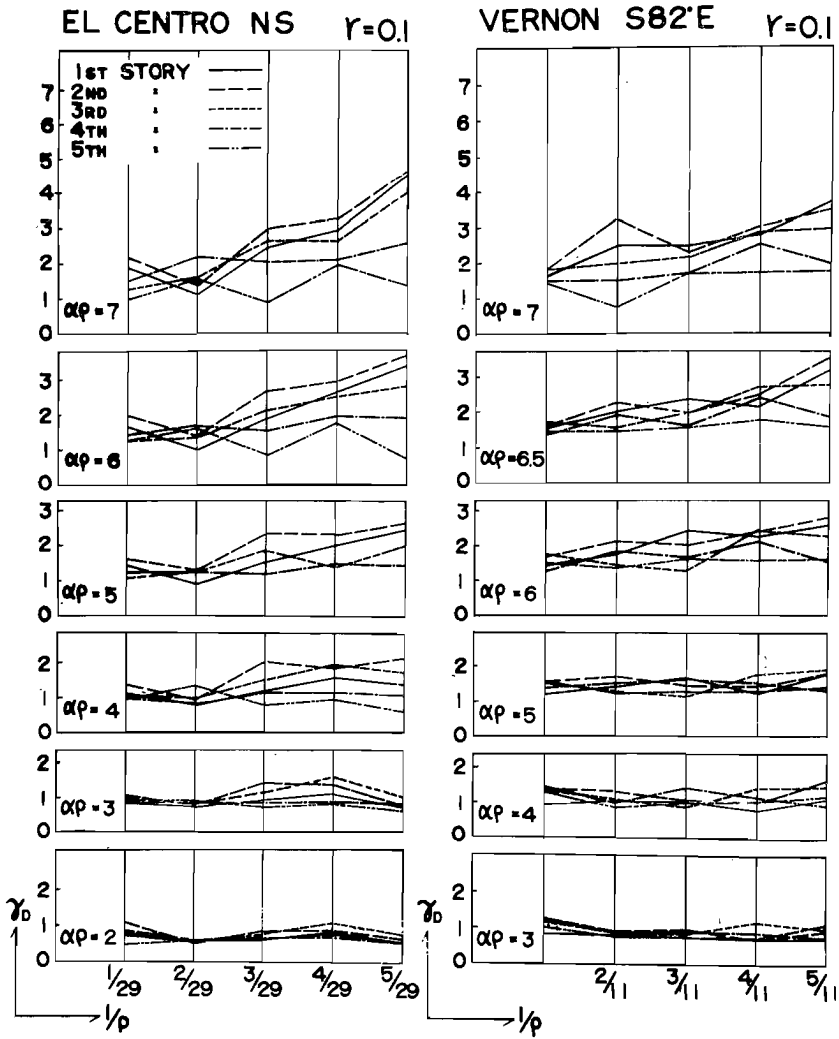


Fig. 14. Basic Response Diagrams of Maximum Ductility Factor-El Centro N-S and Vernon S82°E, Structural Model B_I , Rigidity Ratio $r=0.1$.

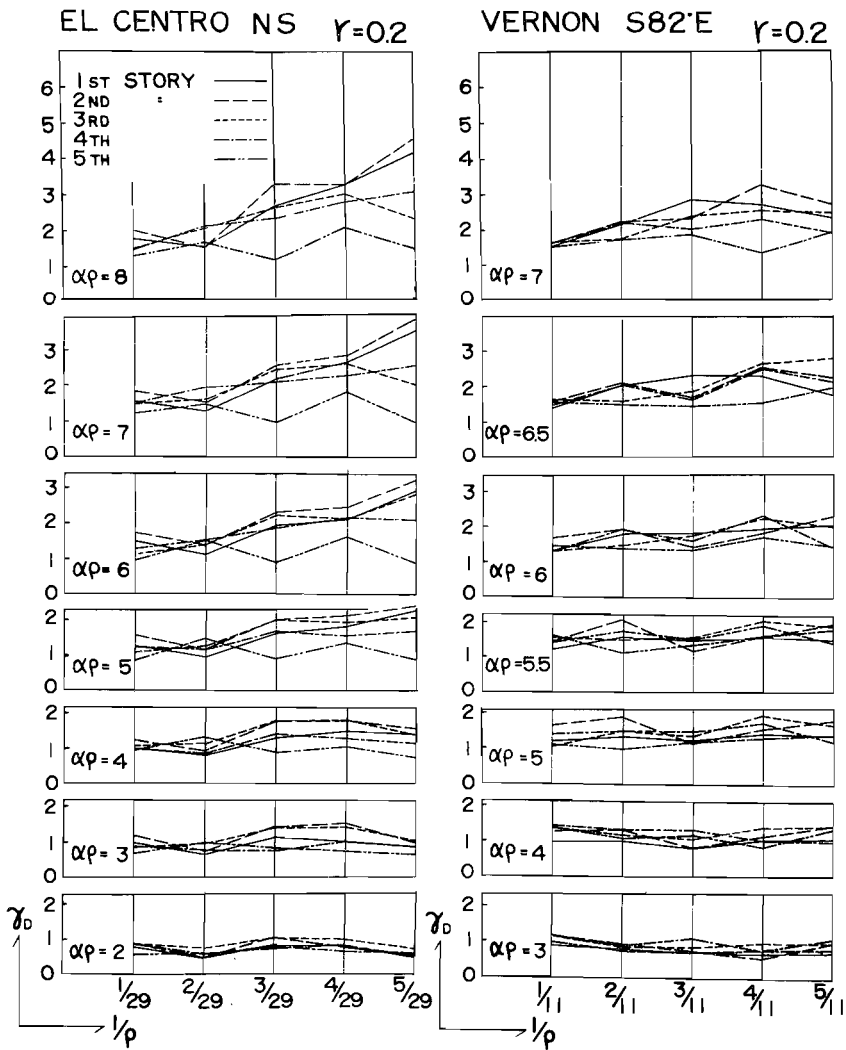


Fig. 15. Basic Response Diagrams of Maximum Ductility Factor-El Centro N-S and Vernon S82°E, Structural Model B_T , Rigidity Ratio $\gamma=0.2$.

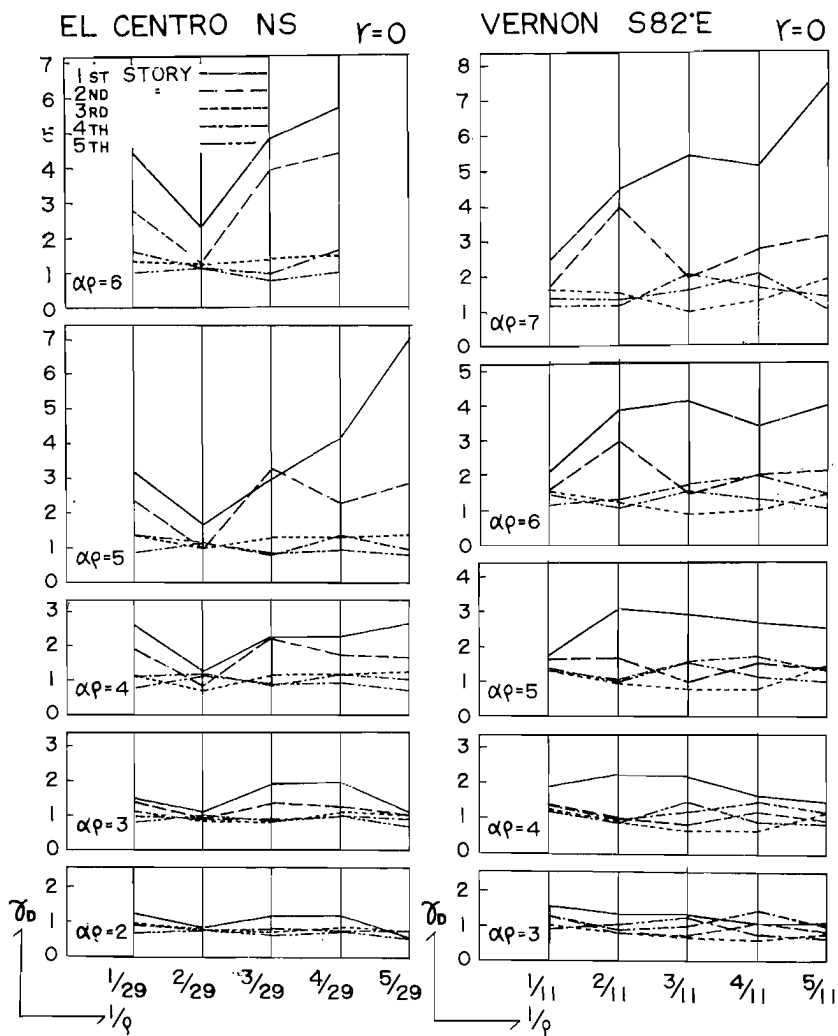


Fig. 16. Basic Response Diagrams of Maximum Ductility Factor-El Centro N-S and Vernon S82°E, Structural Model C_{II} , Rigidity Ratio $\gamma=0$.

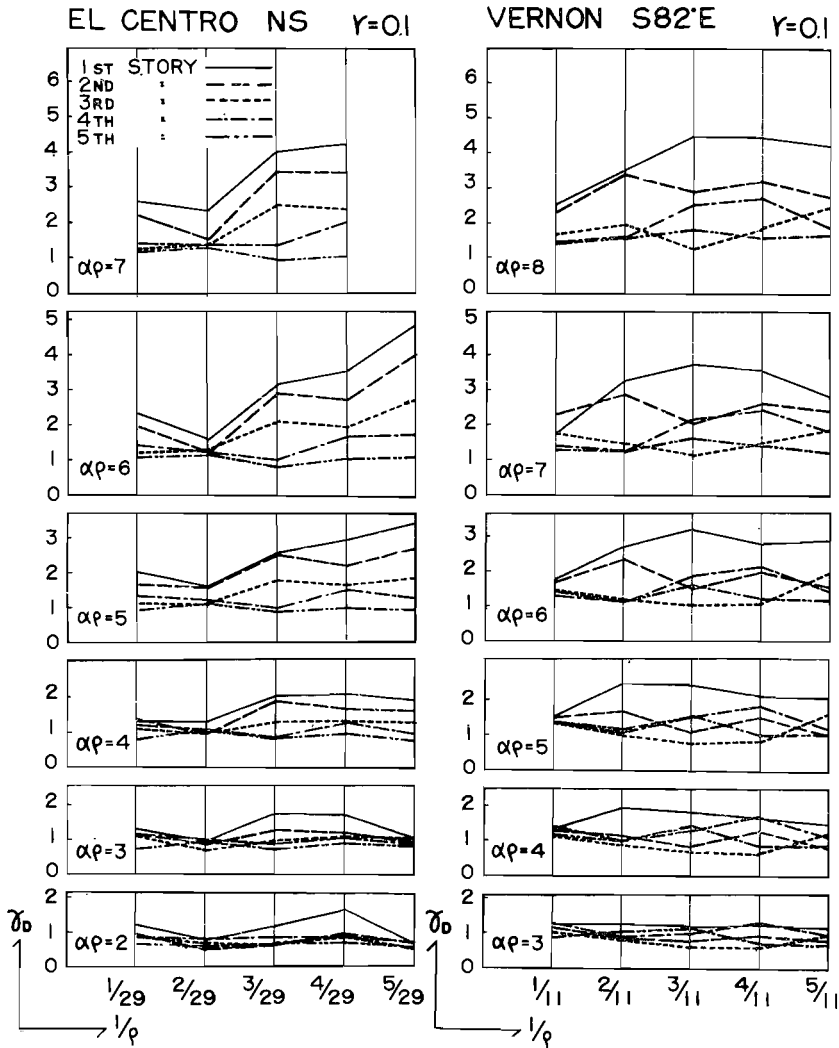


Fig. 17. Basic Response Diagrams of Maximum Ductility Factor-El Centro N-S and Vernon S82°E, Structural Model C_{II} , Rigidity Ratio $r=0.1$.

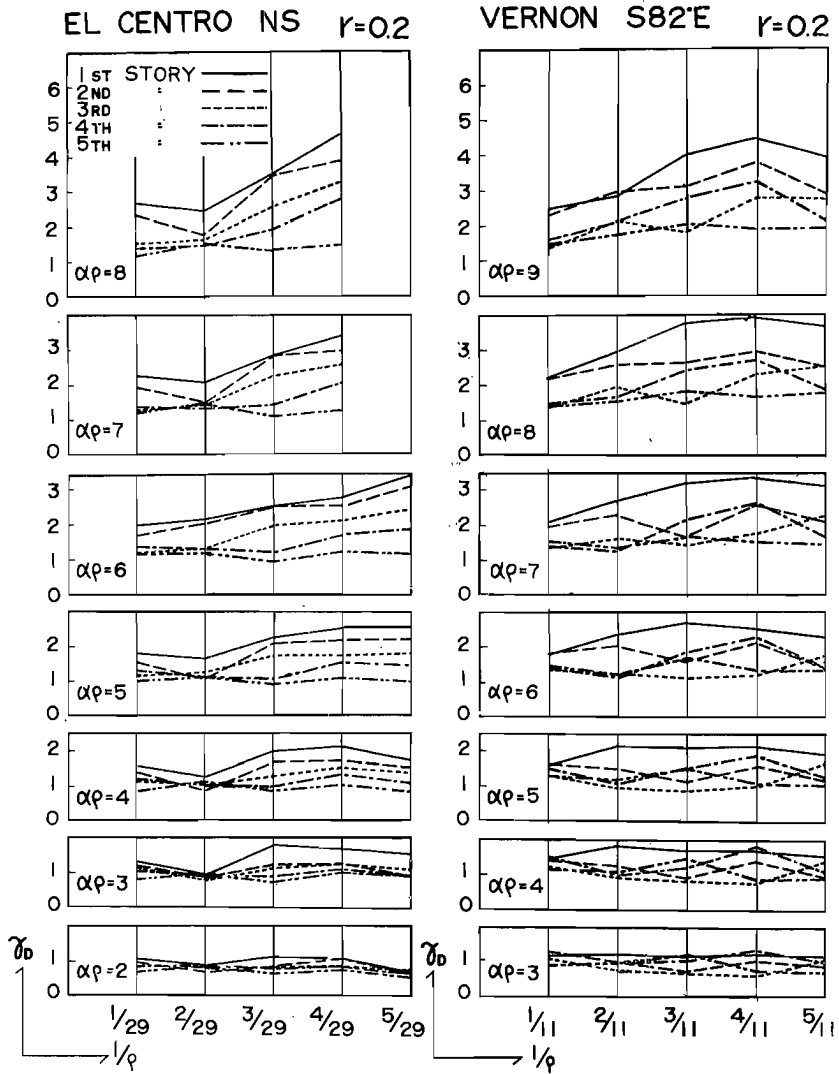


Fig. 18. Basic Response Diagrams of Maximum Ductility Factor-El Centro N-S and Vernon S82°E, Structural Model C_{II} , Rigidity Ratio $r=0.2$.

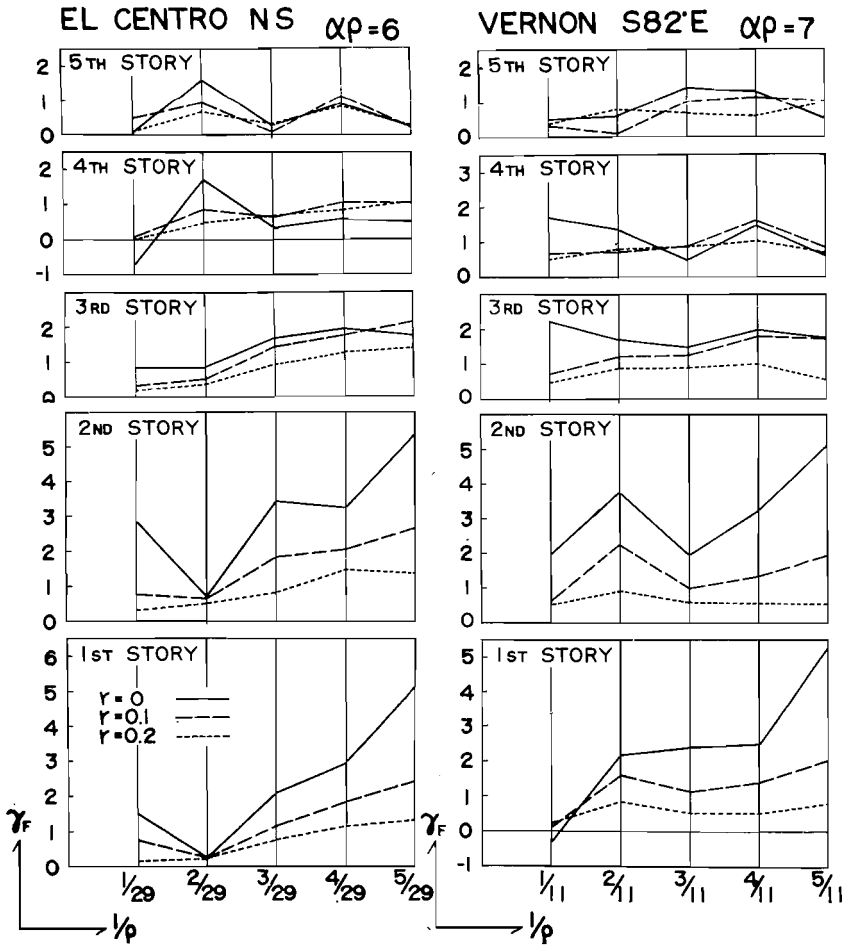


Fig. 19. Response Diagrams of Offset Factor-El Centro N-S and Vernon S82°E, Structural Model B_1 .

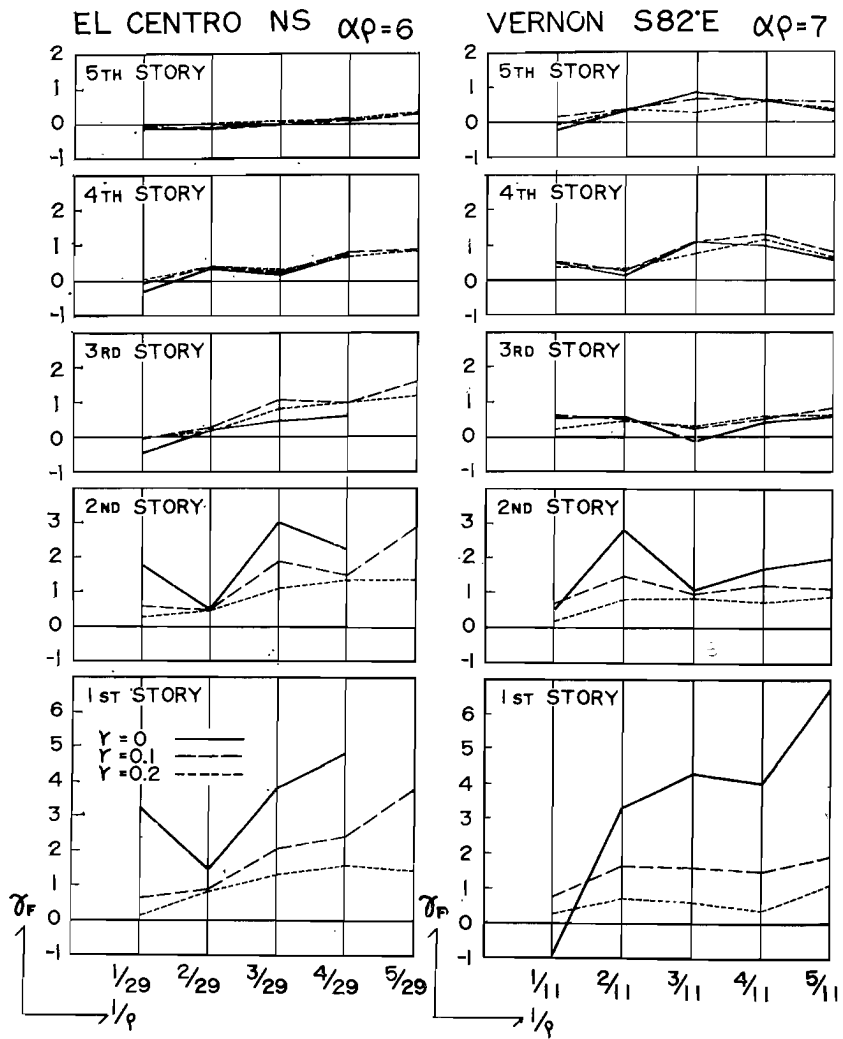


Fig. 20. Response Diagrams of Offset Factor-El Centro N-S and Vernon S82°E, Structural Model C_{II}.

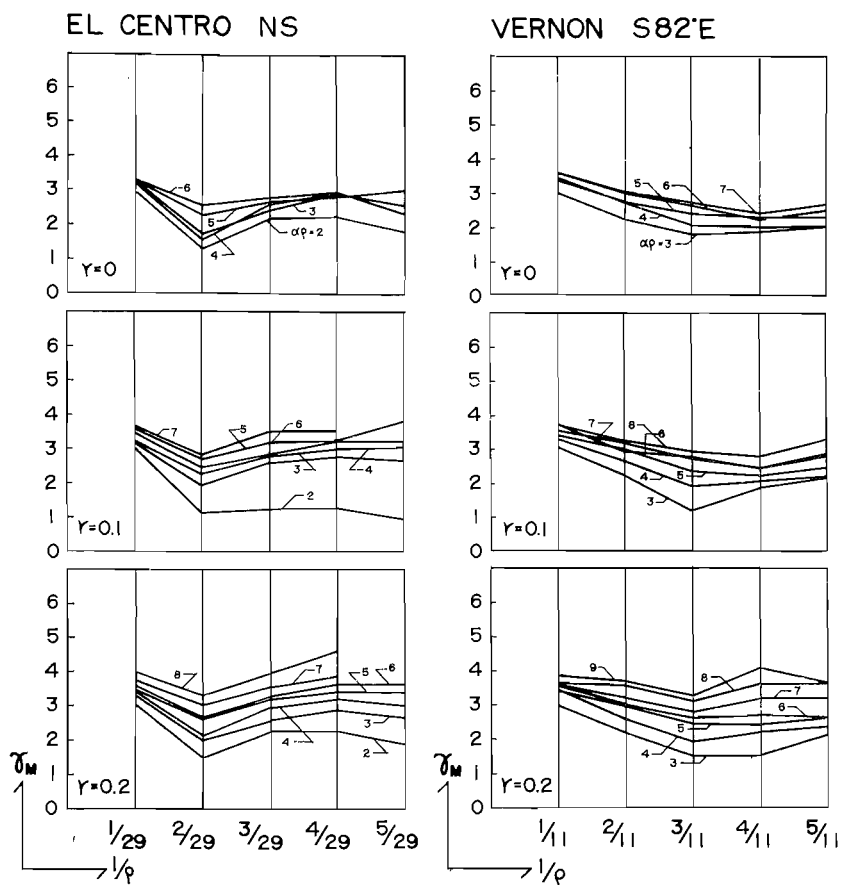


Fig. 21. Response Diagrams of Maximum Overturing Moment Factor-El Centro N-S and Vernon S82°E, Structural Model C_{II} .

The maximum overturning moment factor γ_M and its variance with respect to ν , on the contrary, are increasing functions of ν . This fact may be concerned to the following inequality.

$$\gamma_M \leq \sum_{j=1}^n l_j \beta_j [1 + \nu_j (\gamma_{aj} - 1)] \quad (20)$$

In this analysis, γ_M seems to be a weak function of ν , ρ^{-1} and ν . And its value is in the range, 75%~100% of the upper bound in the case $\nu=0$, $\{l_j\}=\{1\}$ and $n=5$, i.e. the sum of β_j 's. Regardless of the wave shape functions, the El Centro type and the Vernon type, there is such a trend that the responses of B_I and C_{II} models are dispersing and those of the lower stories are particularly increasing as both values of ν and ρ^{-1} are larger. This trend must be considerably restrained by the introduction of the slightly positive parameter ν . It is noticed that the non-dimensional wave shape functions have little effect on the above-mentioned qualitative characteristics of the earthquake responses though they have considerable effect on the quantitative characteristics of the responses, as found in the following sections.

4. Optimum dynamic characteristics

4.1 The optimum dynamic characteristics for a excitation group can be defined by the following conditional minimum value problem, considering the maximum ductility factor γ_D as the most important basic response of the structural system.

$$I = \frac{1}{n} \sum_{j=1}^n \nu_j^2 \left(\gamma_{aj} - \frac{\tilde{\gamma}_{aj}}{\nu_j} \right)^2 \quad (21)$$

$$\max_j \frac{\tilde{\gamma}_{aj}}{\nu_j} = \gamma_a \quad j = 1, 2, \dots, n. \quad (22)$$

where $\{\tilde{\gamma}_{aj}\}$ represents the maximum of $\{\gamma_{aj}\}$ to the excitation group. $\{\nu_j\}$ is the distribution vector of the allowable values of the ductility factor $\{\gamma_{aj}\}$, and γ_a is the corresponding standard value. Namely

$$\{\gamma_{a \text{ allow. } j}\} = \{\gamma_{a \text{ ult. } j} / A_{Rj}\} = \gamma_a \{\nu_j\} \quad (23)$$

where $\gamma_{a \text{ allow. } j}$ and $\gamma_{a \text{ ult. } j}$ denote the allowable and ultimate ductility factors of the j -th story respectively, and A_{Rj} is the properly chosen safety factor of the j -th story. This problem is to find the dynamic characteristics $(\bar{M}\{m_j\}, \bar{K}\{\kappa_j\}, \bar{A}\{\delta_j\}, \{\nu_j\})$ so as to make the functional I minimize

under the condition of eq. (22) and of the prescribed excitation group. If an excitation group is given by $A(T_a)$ and $\alpha(\tau)$, $\{\tilde{\gamma}_{aj}\}$ is determined as a function of the dynamic characteristics of the structural model, that is

$$\{\tilde{\gamma}_{aj}\} = \{\tilde{\gamma}_{aj}(\{m_j\}, \{\kappa_j\}, \{\delta_j\}, \{\gamma_j\}; \bar{M}, \bar{K}, \bar{A}; A(T_a), \alpha(\tau))\} \quad (24)$$

As a general rule, the optimum dynamic characteristics should be determined under consideration of the two kinds of excitation groups with different intensities. And the optimum dynamic characteristics should be stable in spite of the wide variations of various parameters with respect to both the structural system and the earthquake excitation, because of the indeterminate property of earthquake excitations and of the structural modifications of the dynamic characteristics under the various actual conditions. Therefore, the dynamic characteristics must be suitable in the appropriately wide domain of the two independent parameters of the non-dimensional earthquake, that is to say, the following formulation may be possible.

$$\left. \begin{aligned} I &= \frac{1}{n} \iint_R \sum_{j=1}^n \nu_j^2 \left(\max_j \frac{\gamma_{aj}}{\nu_j} - \frac{\gamma_{a1}}{\nu_1} \right)^2 ds / \iint_R ds \\ &= \frac{1}{n} \iint_R \gamma_D^2 \sum_{j=1}^n \nu_j^2 (a - n\gamma_{aj})^2 ds / \iint_R ds \\ &\leq \frac{1}{n} \sum_{j=1}^n \nu_j^2 \iint_R \gamma_D^2 (a+b)^2 ds / \iint_R ds \end{aligned} \right\} \quad (25)$$

$$\max_j \left(\frac{\tilde{\gamma}_{aj}}{\nu_j} \right)_k = (\tilde{\gamma}_D^m)_k + (\bar{a})_k (\tilde{\gamma}_D^s)_k \leq (\gamma_a)_k, \quad k=1, 2. \quad (26)$$

where $ds = d\alpha \cdot d\rho^{-1}$ or $ds = dv \cdot d\rho^{-1}$

$$\left. \begin{aligned} \frac{\gamma_{aj}}{\nu_j} &= \gamma_D^m + \gamma_{aj}^a, \quad \gamma_D^m = \frac{1}{n} \sum_{j=1}^n \frac{\gamma_{aj}}{\nu_j}, \quad \gamma_D^s = \left(\frac{1}{n} \sum_{j=1}^n \gamma_{aj}^2 \right)^{1/2} \\ n\gamma_{aj} &= \gamma_{aj}^a / \gamma_D^s, \quad a = \max_j n\gamma_{aj}, \quad b = -\min_j n\gamma_{aj} \end{aligned} \right\} \quad (27)$$

and $\tilde{\gamma}_{aj}/\nu_j$, $\tilde{\gamma}_D^m$, \bar{a} and $\tilde{\gamma}_D^s$ denote each response value due to the most destructive wave of a prescribed excitation group. Subscript k in eq. (26) denotes the classification of excitation groups ($k=1$ or 2 corresponds to the very intense group and the moderately intense group respectively). The equality sign in eq. (22) might be replaced by the inequality sign in eq. (26), since two different excitation groups is to be considered at the same time.

On the other hand, the optimum dynamic characteristics can be separated to two sets of optimum distributions and standard values.

$$\left. \begin{aligned} & [\bar{M}\{m_j\}, \bar{K}\{\kappa_j\}, \bar{A}\{\delta_j\}, r\{\mu_j\}]_{\text{optimum for } k=1, 2} \\ & \sim [[\{m_j\}, \{\kappa_j\}, \{\delta_j\}, r\{\mu_j\}]_{\text{optimum in } R}, \\ & [\bar{M}, \bar{K}, \bar{A}]_{\text{optimum for } k=1, 2}] \end{aligned} \right\} \quad (28)$$

So it may be convenient to discuss separately on the optimum distributions and standard values. The set of the optimum distributions may be defined by eq. (25) and can be determined from the basic response diagrams of the maximum ductility factor γ_D calculated for various non-dimensional structural models and earthquake excitations. In eq. (25) the non-dimensional domain R may be previously determined by the two kinds of standard values of allowable maximum ductility factor and by the roughly estimated interrelations between the fundamental natural period $1T$ of the structure and the two kinds of prescribed excitation groups. In general, $\{\gamma_{a_i}\}$ is a non-dimensional vector function in the form,

$$\{\gamma_{a_i}\} = \{\gamma_{a_i}(\alpha, \rho; \{m_j\}, \{\kappa_j\}, \{\delta_j\}, \{r_j\}; \alpha(\tau))\} \quad (29-a)$$

or

$$\{\gamma_{a_i}\} = \{\gamma_{a_i}(v, \rho; \{m_j\}, \{\kappa_j\}, \{\delta_j\}, \{r_i\}; \alpha(\tau))\} \quad (29-b)$$

each of which corresponds to the intensity parameter α or v . Then the minimum value problem given by eq. (25) can be discussed only in non-dimensional space, and the set of the optimum distributions can be determined so as to minimize the functional I defined in R to a prescribed wave shape function of earthquake excitations. The set of the optimum standard values, on the other hand, can be determined from eq. (26) using the basic response diagram with respect to the above-mentioned optimum distributions. Eq. (26) contains the standard values of the dynamic characteristics and the frequency characteristics of the maximum acceleration amplitude of the excitation group as in eq. (24). Therefore the set of the optimum standard values is determined so that every value of $\max_j(\bar{\gamma}_{a_i}/\nu_i)_k$ for the two different excitation groups remains within the corresponding standard value of the allowable maximum ductility factor $(\gamma_a)_k$. In the above procedure to determine the optimum dynamic characteristics, the optimum distributions are mainly intended to obtain the uniform distribution of aseismic safety, and also the optimum standard values are intended to give the most economical assurance of the prescribed aseismic safety to the structural system. So eq. (25) can be simplified by eq. (30), because the maximum value α and absolute minimum value

b of the normarized random variable $n\gamma_a$, with respect to j are expressed by the random functions of both the parameters of the non-dimensional earthquake and the distribution vectors of the dynamic characteristics.

$$I = \frac{\iint_R \gamma_D^s ds}{\iint_R ds} \leq \max_R \gamma_D^s \quad (30)$$

It may be desirable to choose a weak function of the parameters of the non-dimensional earthquake as the measure of the suitable dynamic characteristics, because the optimum distributions should be determined in the wide domain of the parameters. From this point of view, eq. (30) should be replaced by the following equation,

$$I = \frac{\iint_R (\gamma_D^s / \gamma_D^m) ds}{\iint_R ds} \leq \max_R (\gamma_D^s / \gamma_D^m) \quad (31)$$

whre the functional I is the mean of the standard deviation choosing $(\gamma_D^m)^{-1}$ as the weighting function. Thus the optimum distributions of the dynamic characteristics can be obtained so as to minimize this mean. As the quantity γ_D^s / γ_D^m is a weak function in the domain R , eq. (31) may be roughly estimated by the following quantity.

$$I = \max_R (\gamma_D^s / \gamma_D^m) \quad (32)$$

Or, taking the ratio of the maximum deviation $\alpha\gamma_D^s$ to the mean γ_D^m , we have

$$I = \max_R (\alpha\gamma_D^s / \gamma_D^m) \quad (33)$$

In the engineering sense, the optimum distributions may be considered as the set of the suitable distribution vectors of dynamic characteristics which makes the functional I be smaller than a value ϵ chosen appropriately. Under this consideration to eq. (33), the following inequality may be expected.

$$\max_j \frac{\gamma_{a_j}}{\nu_j} \leq (1 + \epsilon) \gamma_D^m \leq \gamma_a \quad \text{for all points in } R \quad (34)$$

And the optimum standard values defined by eq. (26) are determined by the following procedure. We determine, at first, the superior response of the maximum ductility factor $\{\gamma_{a_j}\}$ divided by the distribution $\{\nu_j\}$ of the allowable value.

$$\sup_j \{\gamma_{a_j} / \nu_j\} = \max_j (\gamma_{a_j} / \nu_j) \quad (35)$$

This quantity is generally a increasing function of the intensity parameter α or v . Making this quantity be equal to the standard value γ_a of the allowable responses, and solving on α or v from this equation, then α or v is expressed as a single-valued function of ρ and γ_a containing γ .

$$\alpha = \alpha(\rho, \gamma_a; \gamma) \quad \text{or} \quad v = v(\rho, \gamma_a; \gamma) \quad (36)$$

And the standard value \bar{M} of mass is assumed to be known here. Considering the fundamental natural period ${}_1T$ as a parameter, the standard value \bar{K} of rigidity and the standard value \bar{B} of strength at the elastic limit can be expressed as follows

$$\bar{K} = \bar{K}({}_1T) = ({}_1\tau/{}_1T)^2 \bar{M} \quad (37)$$

$$\bar{B} = \bar{B}({}_1T, \gamma_a; \gamma) = \max_k \bar{B}_k, \quad \bar{B}_k = \max(\bar{B}_{\hat{a}k}, \bar{B}_{\hat{v}k}, \bar{B}_{\hat{d}k}) \quad (38)$$

In eq. (38). subscripts \hat{a} , \hat{v} and \hat{d} correspond to each sub-group of the supposed excitation group that are characterized by the constant maximum acceleration, velocity and displacement, respectively, and subscript k denotes one of the excitation groups as shown in eq. (26). For simplicity, we will consider hereafter about the very intense excitation group only. Then the subscript k in eq. (38) can be excluded. Choosing α as an intensity parameter, $\bar{B}_{\hat{a}}$, $\bar{B}_{\hat{v}}$ and $\bar{B}_{\hat{d}}$ are obtained by the following equations.

$$\left. \begin{aligned} \bar{B}_{\hat{a}} &= \frac{C_{\hat{a}} \bar{M}}{\min_{\rho < \rho_l} (\alpha)}, & \min_{\rho < \rho_l} (\alpha) &= \min_{\rho < \rho_l} \alpha(\rho, \gamma_a; \gamma) \\ \bar{B}_{\hat{v}} &= \frac{C_{\hat{v}} \bar{M}}{\min_{\rho_l \leq \rho \leq \rho_u} (\alpha \rho) {}_1T}, & \min_{\rho_l \leq \rho \leq \rho_u} (\alpha \rho) &= \min_{\rho_l \leq \rho \leq \rho_u} \alpha(\rho, \gamma_a; \gamma) \rho \\ \bar{B}_{\hat{d}} &= \frac{C_{\hat{d}} \bar{M}}{\min_{\rho_u < \rho} (\alpha \rho^2) {}_1T^2}, & \min_{\rho_u < \rho} (\alpha \rho^2) &= \min_{\rho_u < \rho} \alpha(\rho, \gamma_a; \gamma) \rho^2 \end{aligned} \right\} \quad (39-a)$$

where $\rho_l = T_{a1}/{}_1T$, $\rho_u = T_{au}/{}_1T$

If we take v instead of α , as an intensity parameter eq. (39-a) is replaced by the following equations.

$$\left. \begin{aligned} \bar{B}_{\hat{a}} &= \frac{C_{\hat{a}} \bar{M}}{\min_{\rho < \rho_l} (v \rho^{-1})}, & \min_{\rho < \rho_l} (v \rho^{-1}) &= \min_{\rho < \rho_l} v(\rho, \gamma_a; \gamma) \rho^{-1} \\ \bar{B}_{\hat{v}} &= \frac{C_{\hat{v}} \bar{M}}{\min_{\rho_l \leq \rho \leq \rho_u} (v) {}_1T}, & \min_{\rho_l \leq \rho \leq \rho_u} (v) &= \min_{\rho_l \leq \rho \leq \rho_u} v(\rho, \gamma_a; \gamma) \\ \bar{B}_{\hat{d}} &= \frac{C_{\hat{d}} \bar{M}}{\min_{\rho_u < \rho} (v \rho) {}_1T^2}, & \min_{\rho_u < \rho} (v \rho) &= \min_{\rho_u < \rho} v(\rho, \gamma_a; \gamma) \rho \end{aligned} \right\} \quad (39-b)$$

Eqs. (37)~(39) are based on the fact that $\sup_j \{\gamma_{a1}/\nu_j\}$ is an increasing function of the intensity parameter and that \bar{K} and \bar{B} are independent each other. The partial derivative of $\sup_j \{\gamma_{a1}/\nu_j\}$ with respect to α or v is sectionally continuous and not negative in each range where the continuity is valid. So the following inequality is valid since $\partial\alpha/\partial\bar{B}$ or $\partial v/\partial\bar{B}$ is always negative.

$$\frac{\partial}{\partial\bar{B}} \sup_j \{\gamma_{a1}/\nu_j\} = \frac{\partial}{\partial\alpha} \sup_j \{\gamma_{a1}/\nu_j\} \cdot \frac{\partial\alpha}{\partial\bar{B}} \leq 0 \quad (40-a)$$

$$\text{or} \quad \frac{\partial}{\partial\bar{B}} \sup_j \{\gamma_{a1}/\nu_j\} = \frac{\partial}{\partial v} \sup_j \{\gamma_{a1}/\nu_j\} \cdot \frac{\partial v}{\partial\bar{B}} \leq 0 \quad (40-b)$$

The independence between \bar{K} and \bar{B} may be valid for the composite structure, and then the aseismic structural elements, the earthquake resistant walls or bracings, should be generally applied to the structural system. When the independence is not valid, the relation between \bar{K} and \bar{B} must be prescribed. Under the rough presumption of the properties of a structural system, the incremental relation between \bar{K} and \bar{B} is only to be known. Without loss of generality, we can assume this relation to be linear. That is, the standard value \bar{A} of the relative displacement at the elastic limit may be previously known, corresponding to the number of degrees of freedom of the structural model and to the outlined properties of the original structural system. In this case, both \bar{K} and \bar{B} are determined by the functions of \bar{A} and γ_a containing r as a parameter. Eliminating ${}_1T$ from the following two relations,

$$\left. \begin{aligned} \bar{B} &= \bar{B}({}_1T, \gamma_a; r) \\ \bar{B} &= \bar{K}\bar{A} = ({}_1\tau/{}_1T)^2 \bar{M}\bar{A} \end{aligned} \right\} \quad (41)$$

we obtain

$$\left. \begin{aligned} \bar{B} &= \bar{B}(\bar{A}, \gamma_a; r), \quad \bar{K} = \bar{B}/\bar{A} = \bar{K}(\bar{A}, \gamma_a; r) \\ {}_1T &= {}_1\tau[\bar{M}\bar{A}/\bar{B}]^{1/2} = {}_1T(\bar{A}, \gamma_a; r) \end{aligned} \right\} \quad (42)$$

In eqs. (41) and (42), the following inequality is assumed to be valid in each domain of the continuous partial derivatives.

$$\begin{aligned} \frac{\partial}{\partial\bar{B}} \sup_j \{\gamma_{a1}/\nu_j\} &= \left(\frac{\alpha}{\partial\alpha} \sup_j \{\gamma_{a1}/\nu_j\} \frac{\partial f_c}{\partial\rho} + \frac{\partial}{\partial\rho} \sup_j \{\gamma_{a1}/\nu_j\} \right) \frac{\partial\rho}{\partial\bar{B}} \\ &+ \frac{\alpha}{\partial\alpha} \sup_j \{\gamma_{a1}/\nu_j\} \frac{\partial f_c}{\partial\bar{B}} \leq 0 \end{aligned} \quad (43)$$

where

$$\sup_j \{\gamma_{a1}/\nu_j\} = \sup_j \{\gamma_{a1}(\alpha, \rho; r)/\nu_j\}$$

$$f_c = f_c(\rho, \bar{B}) = A(\rho_1 \tau [\bar{M}\bar{A}/\bar{B}]^{1/2}) \bar{M}/\bar{B}$$

or

$$\frac{\partial}{\partial \bar{B}} \sup_j \{\gamma_{a_j} \nu_j\} = \left(\frac{\partial}{\partial v} \sup_j \{\gamma_{a_j} \nu_j\} \frac{\partial f_c}{\partial v} + \frac{\partial}{\partial \rho} \sup_j \{\gamma_{a_j} \nu_j\} \right) \frac{\partial \rho}{\partial \bar{B}} + \frac{\partial}{\partial v} \sup_j \{\gamma_{a_j} \nu_j\} \frac{\partial f_c}{\partial \bar{B}} \leq 0 \quad (44)$$

where

$$\sup_j \{\gamma_{a_j} \nu_j\} = \sup_j \{\gamma_{a_j}(v, \rho; r) \nu_j\}$$

$$f_c = f_c(\rho, \bar{B}) = A(\rho_1 \tau [\bar{M}\bar{A}/\bar{B}]^{1/2}) \rho \bar{M}/\bar{B}$$

The other standard values \bar{A} and \bar{E} , and also the standard value \bar{P} of the allowable elasto-plastic potential energy $\{P_j\}$ can be determined by substituting eqs. (37), (38) or (42) corresponding to the relation between \bar{K} and \bar{B} , into the following equations.

$$\left. \begin{aligned} \bar{A} = \frac{\bar{B}}{\bar{K}} = \frac{\bar{B}_1 T^2}{\bar{M}_1 \tau^2}, \quad \bar{E} = \frac{\bar{B}\bar{A}}{2} = \frac{\bar{B}^2 T^2}{2\bar{M}_1 \tau^2} \\ \bar{P} = [2\gamma_a - 1 + r(\gamma_a - 1)^2] \bar{E} = [2\gamma_a - 1 + r(\gamma_a - 1)^2] \frac{\bar{B}^2 T^2}{2\bar{M}_1 \tau^2} \end{aligned} \right\} \quad (45)$$

Consequently the optimum dynamic characteristics of the structural model with the bi-linear hysteretic characteristics are completely determined as a set of the following vectors.

$$\left. \begin{aligned} \{M_j\} = \bar{M}\{m_j\}, \quad \{K_{1j}\} = \bar{K}\{\kappa_j\}, \quad \{K_{2j}\} = \bar{K}\{r_j \kappa_j\} = \bar{K}r\{\mu_j \kappa_j\} \\ \{A_j\} = \bar{A}\{\delta_j\}, \quad \{B_j\} = \bar{B}\{\beta_j\} = \bar{B}\{\kappa_j \delta_j\}, \quad \{E_j\} = \bar{E}\{e_j\} = \bar{E}\{\kappa_j \delta_j^2\} \\ \{P_j\} = \bar{P}\{p_j\} = \bar{P} \left\{ \kappa_j \delta_j^2 \frac{2\gamma_a \nu_j - 1 + r\mu_j (\gamma_a \nu_j - 1)^2}{2\gamma_a - 1 + r(\gamma_a - 1)^2} \right\} \end{aligned} \right\} \quad (46)$$

Since $\{M_j\} = \bar{M}\{m_j\}$ and $\{\gamma_{a_j} \nu_j\} = \gamma_a \{\nu_j\}$ may be considered as the known vectors, at most three vectors are mutually independent among the six unknown vectors $\bar{K}\{\kappa_j\}$, $\bar{A}\{\delta_j\}$, $\bar{B}\{\beta_j\}$, $\bar{E}\{e_j\}$, $\bar{P}\{p_j\}$ and $\{r_j\} = r\{\mu_j\}$. The optimum distributions of dynamic characteristics are provided with three independent non-dimensional vectors, for instance $\{\kappa_j\}$, $\{\beta_j\}$ and $r\{\mu_j\}$, corresponding to the known non-dimensional vectors $\{m_j\}$ and $\gamma_a \{\nu_j\}$'s. If the optimum distributions can be found out, only two independent standard values of the optimum dynamic characteristics should be determined. These standard values are arbitrary two elements of a set of the optimum standard values $[\bar{K}, \bar{A}, \bar{B}, \bar{E}, \bar{P}]$ which corresponds to $\bar{M}\{m_j\}$ and $\gamma_a \{\nu_j\}$'s. If ${}_1T$ or \bar{A} is given, the independent standard value might be reduced to one of \bar{B} , \bar{E} and \bar{P} . It may be convenient for the design data to replace \bar{B} by the so-called base shear coefficient s .

$$s = \frac{B_1}{W_T} = \frac{\bar{B}}{g\bar{M}_T} = \frac{\bar{B}}{g\bar{M}\sum_{j=1}^n m_j} = \frac{A}{g\alpha\sum_{j=1}^n m_j} = \frac{AT_d}{g_1Tv\sum_{j=1}^n m_j} \quad (47)$$

where g is the acceleration of gravity. W_T and M_T are total mass and total weight, respectively. From eqs. (36), (38), (39) and (47), the base shear coefficient s can be determined as a function of ${}_1T$ and γ_a , containing r .

$$s = \max(s_{\hat{a}}, s_{\hat{v}}, s_{\hat{d}}) \quad (48)$$

provided with

$$\left. \begin{aligned} s_{\hat{a}} &= s_{\hat{a}}({}_1T, \gamma_a; r) = \frac{C_{\hat{a}}}{\min_{\rho < \rho_l} (\alpha)g\sum_{j=1}^n m_j} \\ s_{\hat{v}} &= s_{\hat{v}}({}_1T, \gamma_a; r) = \frac{C_{\hat{v}}}{\min_{\rho_l \leq \rho \leq \rho_u} (\alpha\rho)g_1T\sum_{j=1}^n m_j} \\ s_{\hat{d}} &= s_{\hat{d}}({}_1T, \gamma_a; r) = \frac{C_{\hat{d}}}{\min_{\rho_u < \rho} (\alpha\rho^2)g_1T^2\sum_{j=1}^n m_j} \end{aligned} \right\} \quad (49-a)$$

or

$$\left. \begin{aligned} s_{\hat{a}} &= s_{\hat{a}}({}_1T, \gamma_a; r) = \frac{C_{\hat{a}}}{\min_{\rho < \rho_l} (v\rho^{-1})g\sum_{j=1}^n m_j} \\ s_{\hat{v}} &= s_{\hat{v}}({}_1T, \gamma_a; r) = \frac{C_{\hat{v}}}{\min_{\rho_l \leq \rho \leq \rho_u} (v)g_1T\sum_{j=1}^n m_j} \\ s_{\hat{d}} &= s_{\hat{d}}({}_1T, \gamma_a; r) = \frac{C_{\hat{d}}}{\min_{\rho_u < \rho} (v\rho)g_1T^2\sum_{j=1}^n m_j} \end{aligned} \right\} \quad (49-b)$$

In the same way, \bar{E} and \bar{P} can be replaced by the standard values of equivalent relative velocities. \bar{V}_e and \bar{V}_{ev} respectively.

$$\left. \begin{aligned} \frac{\bar{E}}{\bar{M}} &= \frac{1}{2}\bar{V}_e^2, \quad \bar{V}_e = \bar{V}_e({}_1T, \gamma_a; r) = \frac{s_1Tg\sum_{j=1}^n m_j}{1\tau} \\ \frac{\bar{P}}{\bar{M}} &= \frac{1}{2}\bar{V}_{ev}^2, \quad \bar{V}_{ev} = \bar{V}_{ev}({}_1T, \gamma_a; r) = [2\gamma_a - 1 + r(\gamma_a - 1)^2]^{1/2} \frac{s_1Tg\sum_{j=1}^n m_j}{1\tau} \end{aligned} \right\} \quad (50)$$

And also, we can introduce the following quantities for \bar{E} and \bar{P} .

$$e_e = e_e({}_1T, \gamma_a; r) = \frac{\bar{E}}{\bar{W}} = \frac{1}{2g}\bar{V}_e^2 = \frac{1}{2} \left(\frac{s_1T\sum_{j=1}^n m_j}{1\tau} \right)^2 g$$

$$\begin{aligned}
e_{ev} = e_{ev}(1T, \gamma_a ; r) &= \frac{\bar{P}}{\bar{W}} = \frac{1}{2g} \bar{V}_{ev}^2 = \frac{2\gamma_a - 1 + r(\gamma_a - 1)^2}{2} \left(\frac{s_1 T \sum_{j=1}^n m_j}{i\tau} \right)^2 \cdot g \\
p_e = p_e(1T, \gamma_a ; r) &= \frac{E_x}{W_x} = \frac{\sum_{j=1}^n E_j}{\sum_{j=1}^n W_j} = \frac{\bar{E}}{\bar{W}} \frac{\sum_{j=1}^n e_j}{\sum_{j=1}^n m_j} = \frac{1}{2g} \bar{V}_e^2 \frac{\sum_{j=1}^n \beta_j \delta_j}{\sum_{j=1}^n m_j} \\
&= \frac{1}{2} \left(\frac{s_1 T \sum_{j=1}^n m_j}{i\tau} \right)^2 g \frac{\sum_{j=1}^n \kappa_j^{2c-1}}{\sum_{j=1}^n m_j}
\end{aligned} \tag{51}$$

$$\begin{aligned}
p_{ev} = p_{ev}(1T, \gamma_a ; r) &= \frac{P_x}{W_x} = \frac{\sum_{j=1}^n P_j}{\sum_{j=1}^n W_j} = \frac{\bar{P}}{\bar{W}} \frac{\sum_{j=1}^n p_j}{\sum_{j=1}^n m_j} = \frac{1}{2g} \bar{V}_{ev}^2 \frac{\sum_{j=1}^n p_j}{\sum_{j=1}^n m_j} \\
&= \frac{1}{2} \left(\frac{s_1 T \sum_{j=1}^n m_j}{i\tau} \right)^2 g \frac{\sum_{j=1}^n \kappa_j^{2c-1} (2\gamma_a \nu_j - 1 + r \mu_j (\gamma_a \nu_j - 1)^2)}{\sum_{j=1}^n m_j}
\end{aligned} \tag{52}$$

where W_j and \bar{W} are the weight of the j -th mass and its standard value. E_x and P_x are the total elastic potential energy at the elastic limit and the total allowable elasto-plastic potential energy. And so e_e and e_{ev} can be designated as the elastic potential energy factor and the allowable elasto-plastic potential energy factor, respectively. And also p_e and p_{ev} can be called as the total elastic potential energy coefficient and the total allowable elasto-plastic potential energy coefficient respectively. If we substitute the third equation of (42) into eqs. (49)~(52), s , \bar{V}_e , \bar{V}_{ev} , e_e , e_{ev} , p_e and p_{ev} can be expressed by the functions of \bar{A} , γ_a and r . However, it is noticed that these quantities — s , \bar{V}_e , \bar{V}_{ev} , e_e , e_{ev} , p_e and p_{ev} — can be considered to be hardly influenced by the idealization of the structural model, for instance, the number of degrees of freedom of the specific model.

4.2 From Figs. 7~10, it is found that the models of B_I and C_{II} type to the El Centro type excitation group may have the optimum distributions at least in the domain $\alpha \leq 1.0$, $\rho < 35$ ($\gamma_a < 10$) and $\alpha \leq 1.0$, $\rho < 35$ ($\gamma_a < 8$), respectively, under the assumption of the uniform distribution $\{\nu_j\} = \{1\}$ of the allowable ductility factor. The base shear coefficient s corresponding to B_I and C_{II} type can be obtained from eqs. (48), (49-a) at $\{m_j\} = \{1\}$, $n=3$, and eq. (6-b) to the very intense excitation group with the El

Centro type wave shape function. To find general character of the base shear coefficient s , it is assumed here that the maximum ductility factor γ_D in the ranges $\rho < 15$ and $\rho > 50$ is constant. For $\rho < 15$, the lower harmonic responses are excited by the low frequency power as well as the higher harmonic responses by the peak frequency power of the supposed acceleration excitation. While, for $\rho > 50$, the lower harmonic responses are mainly excited by the higher frequency power over the peak frequency. When γ_T varies from the small value to the large value, the main range $15 \leq \rho \leq 50$ falls successively into the ranges characterized by the constant maximum acceleration, velocity and displacement amplitude. Supposing that the main range falls separately into the above-mentioned frequency characteristics, the base shear coefficients $s_{\bar{a}}$, $s_{\bar{v}}$ and $s_{\bar{d}}$ obtained by eqs. (49-a) and (6-b) are shown in Fig. 22. In general, these coefficients seem to be the decreasing functions of γ_d , and their absolute rate with respect to γ_d decreases when γ_d becomes larger, although such a trend is

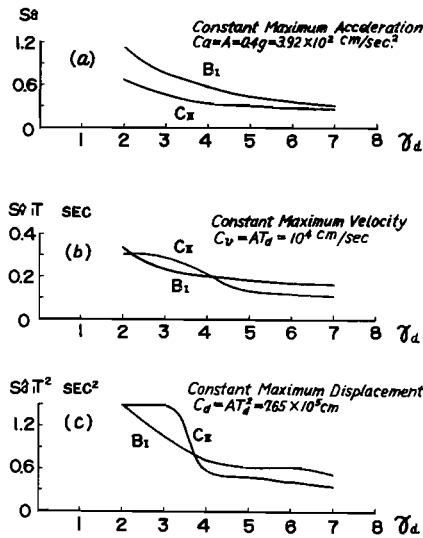


Fig. 22. Base Shear Coefficients $s_{\bar{a}}$, $s_{\bar{v}}$ and $s_{\bar{d}}$ Based on Maximum Ductility Factor in $15 \leq \rho \leq 50$ -El Centro N-S, Structural Models B_I and C_{II} .

different in details, for the type of structural system. To find the interrelation between the maximum ductility factor γ_D and the total dissipated hysteretic energy factor γ_E , we define the superior of the total dissipated hysteretic energy factor as $\sup_j \{\gamma_{ej}/\nu_j\} = \max_j \{\gamma_{ej}/\nu_j\}$, and then we estimate the value $\tilde{\gamma}_e$ at the solution (α, ρ) of the follow-

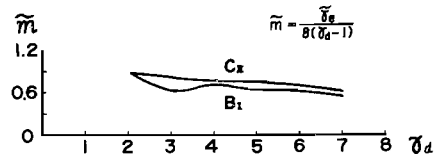


Fig. 23. Equivalent Cycle Number of Hysteresis of $\tilde{\gamma}_e$ for $C_v = 10^4 \text{ cm/sec}$ -El Centro N-S, Structural Models B_I and C_{II} .

ing equation.

$$\sup_j \{\gamma_{ej}/\nu_j\} = \gamma_a \tag{53}$$

This solution of eq. (53) means the most destructive element of the earthquake excitation group. Calculating $\bar{\gamma}_e$ from Figs. 11 and 12 to the group of the constant maximum velocity, we can show, in Fig. 23, the equivalent cycle number of hysteresis \bar{m} which is defined as the ratio of the total dissipated hysteretic energy $\bar{\gamma}_e \bar{B} \bar{A} / 2$ to the hysteretic energy in one cyclic loop of the amplitude $\gamma_a \bar{A}$, that is

$$\bar{m} = \bar{\gamma}_e / 8(\gamma_a - 1) \quad (54)$$

From Fig. 23, it is found that the total dissipated hysteretic energy is not so greater than the energy in one cyclic loop of the amplitude $\gamma_a \bar{A}$ as far as $\gamma_a \geq 2$. On this fact it is based to consider the ductility factor as the primarily important measure of aseismic safety. The base shear coefficient s in the whole range of ${}_1T$ is obtained approximately by the following process. At first, we can determine the value of s at the point $\rho = 50$, when ${}_1T$ is small. This value is equal to previously obtained s_a . Secondary we determine the value of s in the main range $15 \leq \rho \leq 50$ when ${}_1T$ is intermediate. This value of s is submitted to s_b . Finally when ${}_1T$ is large, we determine the value of s in the range $\rho < 15$ from the constant maximum acceleration characteristics without referring to s_a . The base shear coefficients s for the models for B_I and C_{II} type are obtained using the results in Fig. 22 as shown in Figs. 24 and 25 respectively. Strictly calculating s from eqs. (6-b), (7), (36), (48) and (49-a), the smooth curves may be obtained. In comparison with these smooth curves, the

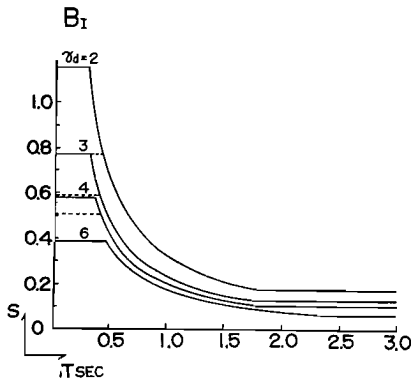


Fig. 24. Base Shear Coefficient for Hypothetical Earthquake Excitation Group-El Centro N-S, Structural Model B_I .

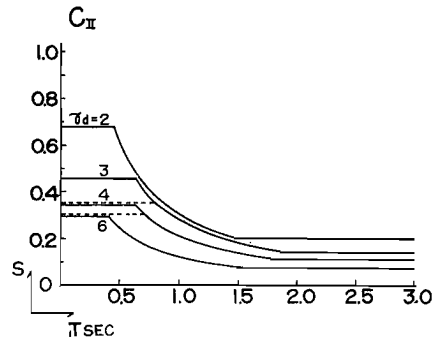


Fig. 25. Base Shear Coefficient for Hypothetical Earthquake Excitation Group-El Centro N-S, Structural Model C_{II} .

full line curves shown in Figs. 24 and 25 may be in safety side on the left side of these figures and in unsafety side on the right side of them. And the dotted lines in Figs. 24 and 25 mean the modified base shear coefficients in the domain where both ${}_1T$ and γ_a are small, considering the internal viscous damping of 5 to 10% critical damping value for the fundamental natural vibration. In these figures, each value of the dotted line levels is estimated from dividing the individual values of the full line levels for $\gamma_a=2, 3, 4$ and 6 by $2/3, (2/3)^{2/3}, (2/3)^{1/3}$ and 1 , respectively^{9,12)}

4.3 We discuss again on the structural models of B_I and C_{II} type with five degrees of freedom and the slightly positive slope of the second bi-linear branch. From the basic response diagrams shown in Figs. 13~18, the mean γ_D^m and the standard deviation γ_D^s defined in eq. (27) are calculated under the assumption of the uniform distribution $\{\nu_j\}=\{1\}$ of the allowable ductility factor. The results for the two different wave shape functions are shown in Figs. 26 and 27 for the models of B_I and C_{II} type respectively. Hence it is considered that the individual models of B_I and C_{II} type may have the optimum distributions when the standard value γ_a is small, but these models can not be optimized if γ_a is large. According to the basic response diagrams in Figs. 13~18, it may be also considered that the slope parameter p defined in eq. (18) is necessary to be larger for the optimum distributions in the case of large γ_a . It is noticed, however, that the effect of the slightly positive rigidity ratio parameter r is especially remarkable to optimize the distributions of dynamic characteristics. The standard deviation γ_D^s is considerably restrained by the slightly positive parameter r as shown in Figs. 26 and 27. On the other hand the mean γ_D^m is a little influenced by the variety of the value of r . The effect of r on γ_D^s increases as γ_D^s is larger, and decreases as r is larger. The base shear coefficient s is calculated from eqs. (7), (36), (48) and (49-b) to the two excitation groups defined by eqs. (6-a) and (6-b). And the calculated results corresponding to the models of B_I and C_{II} type are shown in Figs. 28 and 29. From these figures, it is found that both the wave shape function of excitation group and the optimum dynamic characteristics of structural system have little effect on qualitative characteristics of the base shear coefficient. The base shear coefficient s is generally the decreasing function of ${}_1T, \gamma_a$ and r . And, as either γ_a or r is increasing, s becomes a weak function of ${}_1T$, and also its absolute

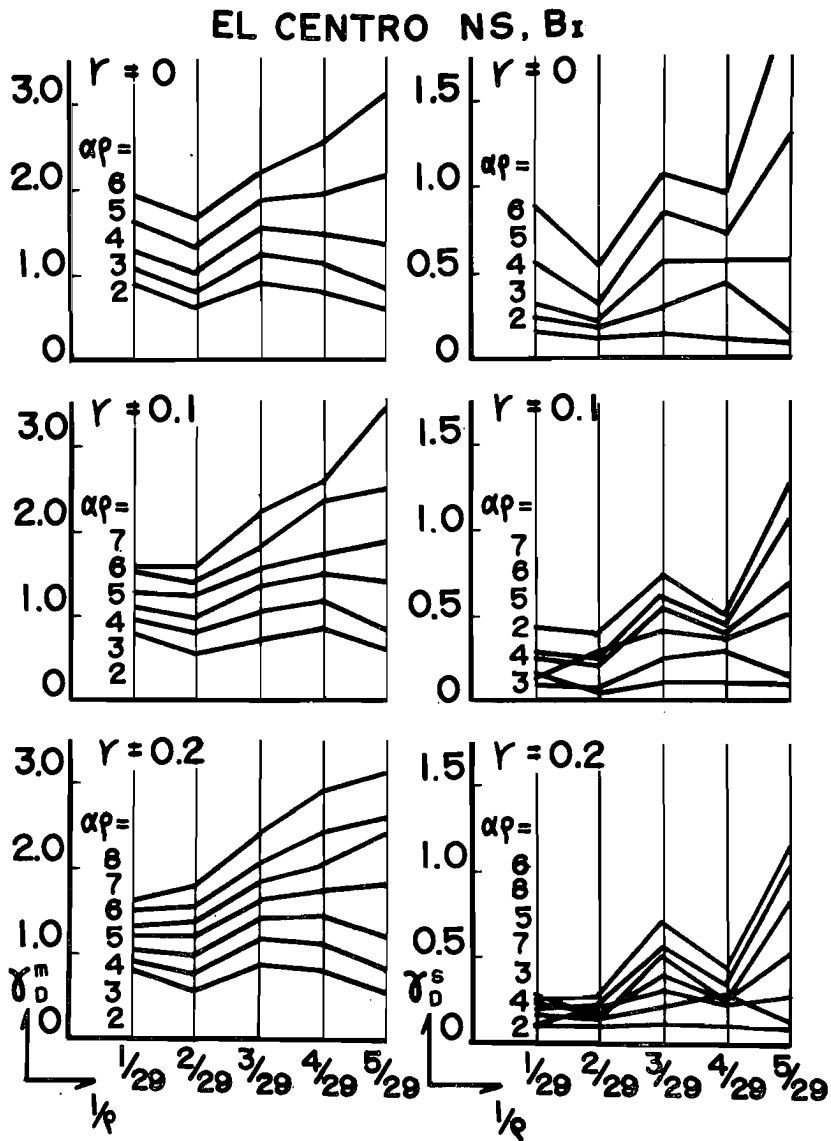


Fig. 26. Mean and Standard Deviation of Standardized Maximum Ductility Factor-El Centro N-S, Structural Model B₁.

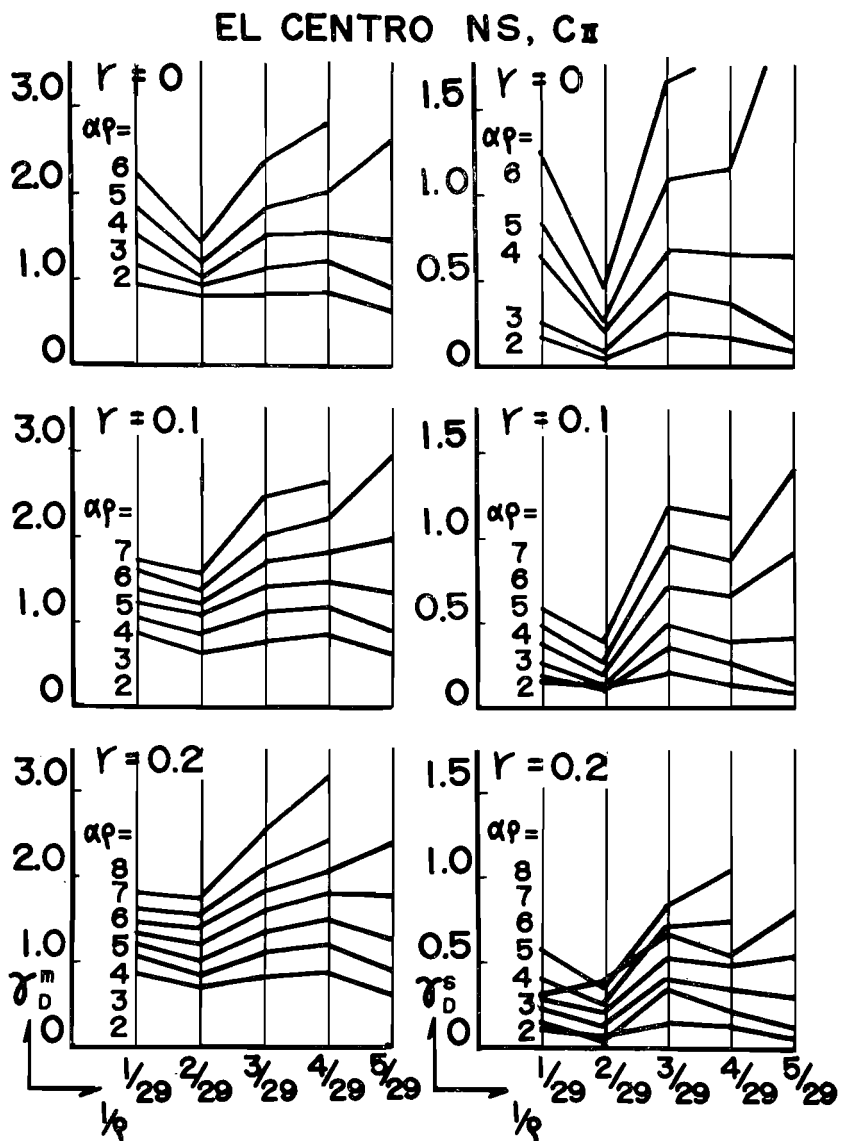


Fig. 27. Mean and Standard Deviation of Standardized Maximum Ductility Factor-El Centro N-S, Structural Model C_{II}.

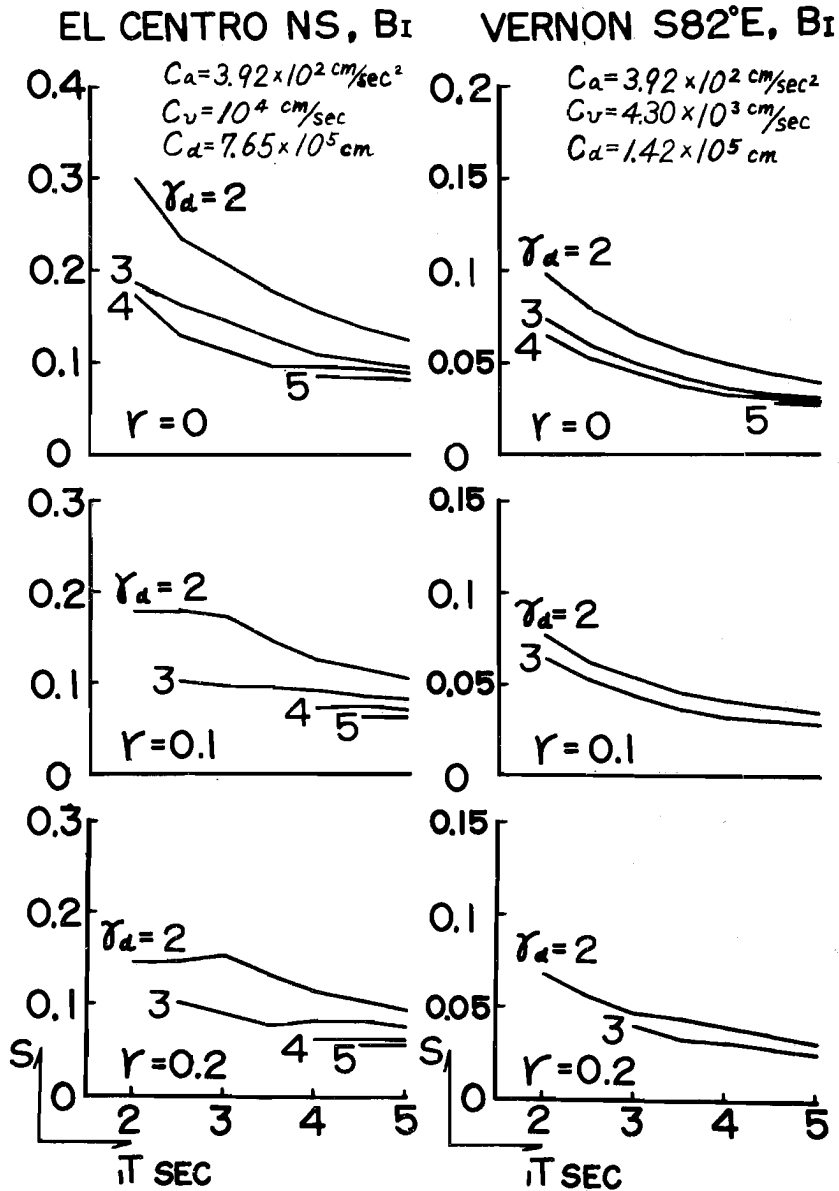


Fig. 28. Base Shear Coefficients for Hypothetical Earthquake Excitation Groups- El Centro N-S and Vernon S82°E, Structural Model B_I.

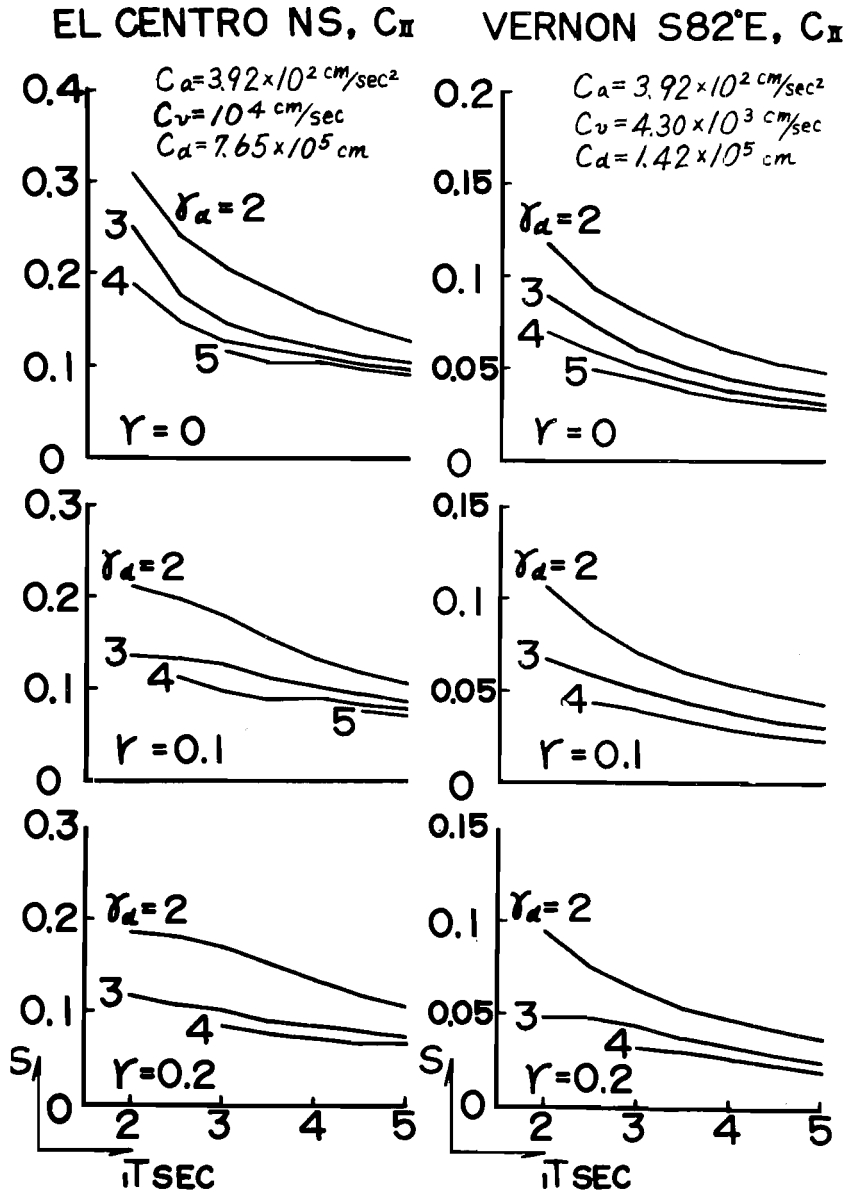


Fig. 29. Base Shear Coefficients for Hypothetical Earthquake Excitation Groups-El Centro N-S and Vernon S82°E, Structural Model C_{II} .

rate with respect to γ_a or r decreases. However the base shear coefficient s for the Vernon type excitation group seems to be smoother than s for the El Centro type. On the other hand, the wave shape function is considerably effective on the base shear coefficient s as to the quantitative characteristics. The base shear coefficient s for the El Centro type has almost two or three times value of s for the Vernon type under each excitation group of the same intensity. Observing the optimum dynamic characteristics, the base shear coefficient s of the model of B_I type seems to be a little smaller than that of C_{II} type, particularly for the Vernon type excitation group. If we try to compare Figs. 28~29 with Figs. 24~25, it is found that the base shear coefficient obtained here is a little larger than that obtained in previous sub-section 4.2 in the range $1T \leq 3$ sec. This fact seems to be mainly caused by the increasing trend of the standard deviation γ_D^s .

5. Aseismic design data

5.1 The aseismic design data for a structure are to be determined from the optimum dynamic characteristics of the structural model. The structural model is assumed to be a n -degrees of freedom system with the uniform distribution of masses. And the optimum dynamic characteristics of the structure with N -degrees of freedom and non-uniform distribution of masses are denoted by

$$\bar{M}_N\{m_j\}_N, \bar{K}_N\{\kappa_j\}_N, \bar{K}_{Nr}\{\mu_j\kappa_j\}_N, \bar{A}_N\{\delta_j\}_N, \bar{B}_N\{\beta_j\}_N, \bar{E}_N\{e_j\}_N, \bar{P}_N\{p_j\}_N$$

where

$$\beta_j = \kappa_j \delta_j, \quad e_j = \beta_j \delta_j, \quad p_j = e_j \frac{2\gamma_a \nu_j - 1 + r \mu_j (\gamma_a \nu_j - 1)^2}{2\gamma_a - 1 + r(\gamma_a - 1)^2} \quad (55)$$

$$j = 1, 2, \dots, N$$

The optimum distributions are determined by the following process. At first, we can obtain the optimum distributions for $\{m\}_N = \{1\}$ from the previously determined optimum distributions by replacing n by N and preserving the characteristics of $\{\mu_j\}$ and $\{\nu_j\}$. And then, considering the assumption that $\{m_j\}_N$ is not so much different from uniform distribution, we determine the optimum distribution $\{\beta_j\}_N$ of the strength at elastic limit under such a condition that the distribution of the shear coefficient is invariable.

$$\left. \begin{aligned} \{\beta_j\}_N = \{f_j \beta_{0j}\}_N, \quad \{f_j\}_N = \left\{ \frac{N}{N-j+1} \cdot \frac{\sum_{j=1}^N m_j}{\sum_{j=1}^N m_j} \right\}_N \\ \{\beta_{0j}\}_N = \{\kappa_{0j}^e\}_N, \quad \{\kappa_{0j}\}_N = \left\{ \frac{2N + p[2(N-j) + 1]}{2N + p[2N-1]} \right\}_N \end{aligned} \right\} \quad (56)$$

where the quantities with subscript 0 correspond to the case of $\{m_j\}_N = \{1\}$. The other several optimum distributions are obtained from eqs. (55) and (56) by supposing the relation $\delta_j = \kappa_j^{e-1}$ or $\delta_j = \kappa_{0j}^{e-1}$. The above each relation corresponds to the fluctuation of mass distribution along the height of structure for the quantity change of densities or areas, because the masses are expressed as the products of densities and areas.

On the other hand, the optimum standard values can be determined as the functions of \bar{M}_N , $\{m_j\}_N$, \bar{A}_N , γ_a , r and N by the following parametric representations with respect to ${}_1T$.

$$\bar{K}_N = ({}_1\tau_N / {}_1T)^2 \bar{M}_N, \quad \bar{B}_N = sg \bar{M}_N \sum_{j=1}^N m_j = s W_T, \quad \bar{A}_N = \bar{B}_N / \bar{K}_N \quad (57-a)$$

$$\bar{E}_N = \bar{B}_N^2 / 2\bar{K}_N, \quad \bar{P}_N = [2\gamma_a - 1 + r(\gamma_a - 1)^2] \bar{B}_N^2 / 2\bar{K}_N \quad (57-b)$$

where

$$\begin{aligned} s = s({}_1T, \gamma_a; r), \quad {}_1\tau_N = {}_1\tau_N(\{m_j\}_N, \{\kappa_j\}_N) \doteq 2\pi \left[\frac{\sum_{j=1}^N m_j j^2}{\sum_{j=1}^N \kappa_j} \right]^{1/2} \\ \bar{A}_N = \bar{L} \theta_e \end{aligned} \quad (58)$$

In eq. (58) the base shear coefficient s is considered as an invariant through the transform of the dynamic characteristics, and the non-dimensional fundamental period ${}_1\tau_N$ determined as a function of the optimum distributions $\{m_j\}_N$ and $\{\kappa_j\}_N$ is approximately expressed by the second equation of (58), assuming that the shape of the fundamental mode is triangular. And \bar{A}_N is considered to be known and expressed by the product of the standard value \bar{L} of the height of interstory and the equivalent rotational angle θ_e of interstory at the elastic limit as shown in eq. (58). Thus the various aseismic design data can be determined from the above-obtained optimum dynamic characteristics. And also the fundamental natural period ${}_1T$ can be expressed as the function of $\{m_j\}_N$, \bar{A}_N , γ_a , r and N by solving the following equation.

$${}_1T^2 = {}_1\tau_N^2 \bar{A}_N / s({}_1T, \gamma_a; r) \cdot g \sum_{j=1}^N m_j \quad (59)$$

The aseismic design data which provide the strength $\{B_j\}_N$ at elastic limit

consist of the base shear coefficient s and the distribution $\{s_j/s\}$ of shear coefficients or the distribution $\{k_j/s\}$ of lateral force coefficients.

$$\{B_j\}_N = s \left\{ \frac{s_j}{s} \sum_{j=j}^N W_j \right\}_N, \quad \frac{s_j}{s} = \frac{\sum_{j=1}^N m_j}{\sum_{j=j}^N m_j} \beta_j = \frac{N}{N-j+1} \beta_{0j} \quad (60)$$

or

$$\left. \begin{aligned} \{B_j\}_N &= s \left\{ \sum_{j=j}^N \frac{k_j}{s} W_j \right\}_N \\ \left\{ \frac{k_j}{s} \right\}_N &= \left\{ \frac{\sum_{j=j}^N m_j}{m_j(N-j+1)} \cdot \frac{k_{0j}}{s} + \frac{\beta_{0j+1}N}{N-j+1} \left[1 - \frac{\sum_{j=j+1}^N m_j}{m_j(N-j)} \right] \right\}_N \end{aligned} \right\} \quad (61)$$

where

$$\left. \begin{aligned} \left\{ \frac{k_{0j}}{s} \right\}_N &= \{(\beta_{0j} - \beta_{0j+1})N\}_N \\ \beta_{0j} &= \kappa_{0j} = \frac{10N - 6j + 3}{10N - 3} \quad \text{for } B_I, \quad \beta_{0j} = 1, \quad \beta_{0N+1} = 0 \\ \beta_{0j} &= \kappa_{0j}^{1/2} = \left[\frac{8N - 6j + 3}{8N - 3} \right]^{1/2} \quad \text{for } C_{II}, \quad j = 1, 2, \dots, N \end{aligned} \right\} \quad (62)$$

and, W_j , s_j and k_j are the weight of the j -th story, shear coefficient and lateral force coefficient, respectively. The aseismic design data to the allowable elasto-plastic potential energy $\{P_j\}_N$ also consist of the standard value of the equivalent relative velocities and their distribution.

$$\begin{aligned} \{P_j\}_N &= \frac{1}{2} \{M_j V_{evj}^2\}_N, \quad \{V_{evj}\}_N = \bar{V}_{evN} \{v_{evj}\}_N, \quad \{v_{evj}\}_N = \{(\rho_j/m_j)^{1/2}\}_N \\ \bar{V}_{evN} &= s [2\gamma_a - 1 + r(\gamma_a - 1)^2]^{1/2} T g \sum_{j=1}^N m_j / 1 \tau_N \end{aligned} \quad (63)$$

Otherwise, assuming that e_{ev} or ρ_{ev} in eq. (51) or (52) is an invariant, $\{P_j\}_N$ can be expressed as follows

$$\{P_j\}_N = e_{ev} \bar{W}_N \{\rho_j\}_N \quad \text{or} \quad \{P_j\}_N = (\rho_{ev} / \sum_{j=1}^N \rho_j) W_T \{\rho_j\}_N \quad (64)$$

And $\{\rho_j\}_N$ can be also expressed by the following equations corresponding to the relation $\delta_j = \kappa_j^{e-1}$ or $\delta_j = \kappa_{0j}^{e-1}$.

$$\left. \begin{aligned} \{\rho_j\}_N &= \left\{ e_j \cdot \frac{2\gamma_a \nu_j - 1 + r \mu_j (\gamma_a \nu_j - 1)^2}{2\gamma_a - 1 + r(\gamma_a - 1)^2} \right\} \\ e_j &= (f_j \kappa_{0j})^{2e-1} \quad \text{for } \delta_j = \kappa_j^{e-1} = \beta_j^{(e-1)/c} \\ e_j &= f_j \kappa_{0j}^{2e-1} \quad \text{for } \delta_j = \kappa_{0j}^{e-1} = \beta_{0j}^{(e-1)/c} \quad j = 1, 2, \dots, N \end{aligned} \right\} \quad (65)$$

If the total number N of stories tends to infinity, the optimum distribution function $\beta(x)$ of the strength at elastic limit can be determined as follows

where $k(x)$ is the lateral force coefficient and x_j is the coordinate corresponding to the $j+1$ -th floor.

The optimum distribution functions of structural models B_I and C_{II} type and the corresponding distribution function of lateral force coefficient in the case that $N \rightarrow \infty$ and $m(x) = 1$, are shown in Figs. 30 and 31, respectively. In Fig. 32 we show the distribution functions of strength and lateral force coefficient in the U.S.A. modern building code⁴. In Fig. 33 we also show the distribution coefficients of the strength at the top story, and compare their coefficient values of the U.S.A. code with the

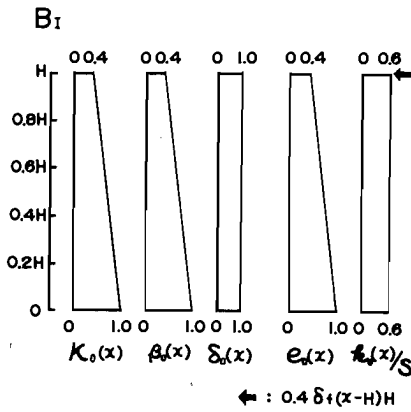


Fig. 30. Optimum Distributions of Dynamic Characteristics and Lateral Force Coefficients-Structural Model B_I .

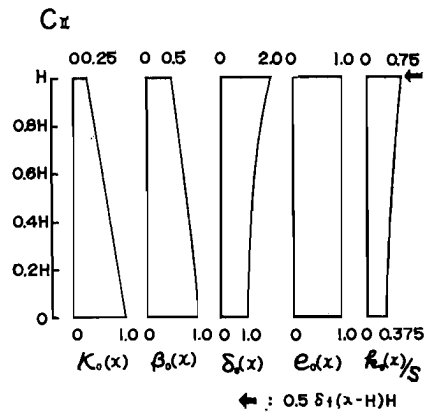


Fig. 31. Optimum Distributions of Dynamic Characteristics and Lateral Force Coefficients-Structural Model C_{II} .

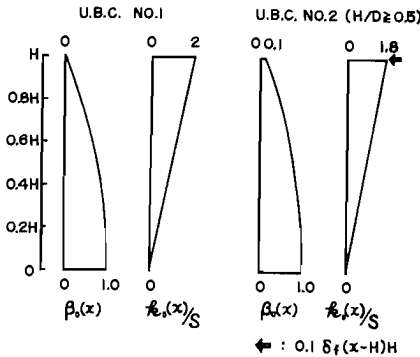


Fig. 32. Distributions of Strength and Lateral Force Coefficients in U.S.A. Modern Code.

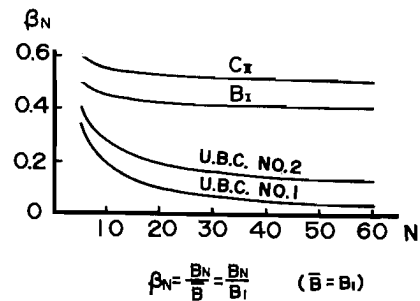


Fig. 33. Distribution Coefficient of Strength at Top Story.

corresponding values obtained here. In these figures, U.B.C. No. 1 denotes the inverse triangular distribution of lateral force coefficient and U.B.C. No. 2 denotes the type of lateral force distribution which consists of the concentrated force of 10% base shear at the top story and the inverse triangular distribution of 90% base shear. And D is the width of the structure. From Fig. 33, it proves that the U.S.A. code gives the characteristics near to the optimum distribution of strength to the low or intermediate building structure, but gives too small value of lateral force to the top story of the tall building structure.

To obtain the numerical values of the aseismic design data expressed in eqs. (60), (63), (64) and (70), it is enough to determine both the base shear coefficient s and the fundamental natural period ${}_1T$, as the explicit functions of the known quantities. This will be discussed in the following sub-sections.

5.2 The base shear coefficients shown in Figs. 24 and 25 can be approximately simplified by the formulas that may be valid for the case $r=0$, $\{\nu_j\}_N=\{1\}$ and the El Centro type wave shape function. Namely

$$\left. \begin{aligned} s_1 &= s_1({}_1T, \gamma_a) = d_1 k(\gamma_a), \quad {}_1T < {}_1T_l \\ s_2 &= s_2({}_1T, \gamma_a) = d_2 k(\gamma_a) {}_1T^{-1}, \quad {}_1T_l \leq {}_1T \leq {}_1T_u \\ s_3 &= s_3({}_1T, \gamma_a) = d_3 k(\gamma_a), \quad {}_1T_u < {}_1T \end{aligned} \right\} \quad (71)$$

where $k(\gamma_a)$ is chosen as simple function of γ_a , and the constants d_1 , d_2 and d_3 are determined so as to minimize the variances with respect to γ_a . The following eqs. (72) and (73) may be applicable to the practical use.

$$k(\gamma_a) = (2\gamma_a - 1)^{1/2} \quad (72-a)$$

$$\left. \begin{aligned} d_1 &= 1.33, \quad d_2 = 0.566 \text{ sec}, \quad d_3 = 0.275, \\ {}_1T_l &= 0.426 \text{ sec}, \quad {}_1T_u = 2.06 \text{ sec} \quad \text{for } B_I \end{aligned} \right\} \quad (72-b)$$

$$\left. \begin{aligned} d_1 &= 0.827, \quad d_2 = 0.492 \text{ sec}, \quad d_3 = 0.292, \\ {}_1T_l &= 0.595 \text{ sec}, \quad {}_1T_u = 1.68 \text{ sec} \quad \text{for } C_{II} \end{aligned} \right\} \quad (72-c)$$

$$k(\gamma_a) = \gamma_a^{1/2} \quad (73-a)$$

$$\left. \begin{aligned} d_1 &= 1.02, \quad d_2 = 0.431 \text{ sec}, \quad d_3 = 0.210, \\ {}_1T_l &= 0.422 \text{ sec}, \quad {}_1T_u = 2.05 \text{ sec} \quad \text{for } B_I \end{aligned} \right\} \quad (73-b)$$

$$\left. \begin{aligned} d_1 &= 0.636, \quad d_2 = 0.376 \text{ sec}, \quad d_3 = 0.224, \\ {}_1T_l &= 0.591 \text{ sec}, \quad {}_1T_u = 1.68 \text{ sec} \quad \text{for } C_{II} \end{aligned} \right\} \quad (73-c)$$

Numerical results of eqs. (72) and (73) are shown in Figs. 34~37, res-

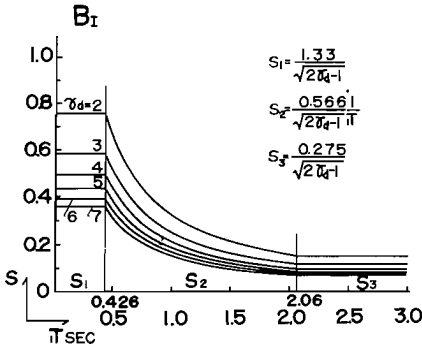


Fig. 34. Simplified Base Shear Coefficient-El Centro N-S, Structural Model B_I .

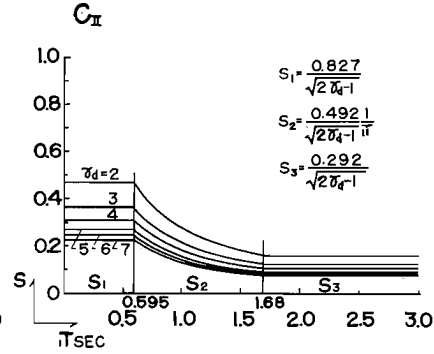


Fig. 35. Simplified Base Shear Coefficient-El Centro N-S, Structural Model C_{II} .

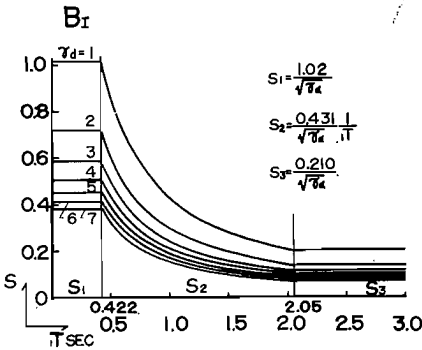


Fig. 36. Simplified Base Shear Coefficient-El Centro N-S, Structural Model B_I .

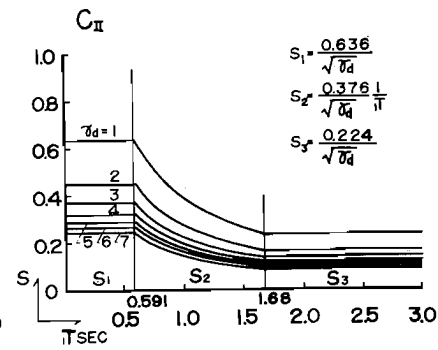


Fig. 37. Simplified Base Shear Coefficient-El Centro N-S, Structural Model C_{II} .

pectively. The fundamental natural period ${}_1T$ can be obtained from eqs. (59) and (71) as a function of \bar{A}_N , N , $\{m_j\}_N$ and $\{\kappa_j\}_N$ as follows

$${}_1T = {}_1T(\bar{A}_N, \gamma_a, N) = \left[\frac{l(\bar{A}_N, N)}{d_i k(\gamma_a)} \right]^{1/2} \quad \text{for } i=1, 3, \quad {}_1T(\bar{A}_N, \gamma_a, N) = \frac{l(\bar{A}_N, N)}{d_2 k(\gamma_a)}$$

where

$$l(\bar{A}_N, N) = \frac{{}_1\tau_N^2 \bar{A}_N}{g \cdot \sum_{j=1}^N m_j}, \quad {}_1\tau_N = {}_1\tau_N(\{m_j\}_N, \{\kappa_j\}_N) \quad (74-b)$$

From eq. (58), the non-dimensional fundamental period ${}_1\tau_N$ is expressed as the second term of the following equation for the case $\{m_j\}_N = \{1\}$ and $\{\kappa_j\}_N$ given by eq. (18).

$${}_1\tau_N \doteq 2\pi \left[\frac{(N+1)(2N+1)[2N+p(2N-1)]}{6N(2+p)} \right]^{1/2} \doteq 2\pi \left[\frac{2}{3} \left(\frac{1+p}{2+p} \right) \right]^{1/2} \cdot N \quad (75)$$

In above equation the third term is valid approximately for considerably large N . Making use of this, eq. (74-b) becomes as follows

$$l(\bar{A}_N, N) = \frac{8\pi^2}{3g} \left(\frac{1+p}{2+p} \right) \bar{A}_N \cdot N = 0.0268 \left(\frac{1+p}{2+p} \right) \bar{A}_N \cdot N \quad (\text{sec}^2), \quad \bar{A}_N \sim (\text{cm}) \quad (76)$$

From eqs. (72), (74) and (76), the fundamental natural period is obtained as follows

$$\begin{aligned} {}_1T &= 0.121(2\gamma_a - 1)^{1/4} (\bar{A}_N \cdot N)^{1/2}, \quad {}_1T < 0.426 \text{ sec} \\ {}_1T &= 0.0339(2\gamma_a - 1)^{1/2} \bar{A}_N \cdot N, \quad 0.426 \text{ sec} \leq {}_1T \leq 2.06 \text{ sec for } B_I \quad (77\text{-a}) \\ {}_1T &= 0.264(2\gamma_a - 1)^{1/4} (\bar{A}_N \cdot N)^{1/2}, \quad 2.06 \text{ sec} < {}_1T, \quad {}_1T \sim (\text{sec}), \quad \bar{A}_N \sim (\text{cm}) \\ {}_1T &= 0.161(2\gamma_a - 1)^{1/4} (\bar{A}_N \cdot N)^{1/2}, \quad {}_1T < 0.595 \text{ sec} \\ {}_1T &= 0.0436(2\gamma_a - 1)^{1/2} \bar{A}_N \cdot N, \quad 0.595 \text{ sec} \leq {}_1T \leq 1.68 \text{ sec for } C_{II} \quad (77\text{-b}) \\ {}_1T &= 0.272(2\gamma_a - 1)^{1/4} (\bar{A}_N \cdot N)^{1/2}, \quad 1.68 \text{ sec} < {}_1T, \quad {}_1T \sim (\text{sec}), \quad \bar{A}_N \sim (\text{cm}) \end{aligned}$$

For instance, the following values are calculated from eq. (77-b).

$$\begin{aligned} C_{II}, \quad \gamma_a = 3, \quad N = 24; \quad \bar{A}_N = 1 \text{ cm} \sim {}_1T = 1.99 \text{ sec}, \quad \bar{A}_N = 2 \text{ cm} \sim {}_1T = 2.82 \text{ sec} \\ \bar{A}_N = 4 \text{ cm} \sim {}_1T = 3.99 \text{ sec} \\ N = 60; \quad \bar{A}_N = 1 \text{ cm} \sim {}_1T = 3.15 \text{ sec}, \quad \bar{A}_N = 2 \text{ cm} \sim {}_1T = 4.46 \text{ sec} \\ \bar{A}_N = 4 \text{ cm} \sim {}_1T = 6.30 \text{ sec} \quad (77\text{-c}) \end{aligned}$$

The standard values \bar{V}_{epN} of the equivalent relative velocity given by eq. (63) are obtained by using eqs. (71) and (72-a) as following expressions.

$$\bar{V}_{epN} = \bar{V}_{epN}({}_1T) = d_{i1} T g \sum_{j=1}^N m_j / {}_1\tau_N, \quad i = 1, 3 \quad (78\text{-a})$$

$$\bar{V}_{epN} = d_{2g} \sum_{j=1}^N m_j / {}_1\tau_N \quad (78\text{-b})$$

And also, the allowable elasto-plastic potential energy factor e_{ep} and the total allowable elasto-plastic potential energy coefficient p_{ep} , which are previously defined by the second equations of (51) and (52), can be determined by the following equations.

$$p_{ep} = \frac{\sum_{j=1}^N p_j}{\sum_{j=1}^N m_j} e_{ep}, \quad \text{where} \quad e_{ep} = \frac{\bar{P}_N}{\bar{W}_N} \quad \text{and} \quad p_{ep} = \frac{P_T}{W_T} \quad (79)$$

$$e_{ep} = e_{ep}({}_1T) = \frac{d_{i1}^2 T^2 g}{2} \left(\frac{\sum_{j=1}^N m_j}{{}_1\tau_N} \right)^2, \quad i = 1, 3 \quad (80\text{-a})$$

$$e_{ev} = \frac{d_2^2}{2} g \left(\frac{\sum_{j=1}^N m_j}{1\tau_N} \right)^2 \quad (80-b)$$

For the case $\{m_j\}_N = \{1\}$ and $\{\nu_j\}_N = \{1\}$, the coefficient $\sum_{j=1}^N p_j / \sum_{j=1}^N m_j$ of eq. (79) becomes

$$\left. \begin{aligned} \frac{\sum_{j=1}^N p_j}{\sum_{j=1}^N m_j} &= \frac{\sum_{j=1}^N p_{0j}}{N} = \frac{(2+p)N}{2N+p(2N-1)}, \quad \text{for } I, (c=1) \\ \frac{\sum_{j=1}^N p_j}{\sum_{j=1}^N m_j} &= \frac{\sum_{j=1}^N p_{0j}}{N} = 1, \quad \text{for } II, \left(c = \frac{1}{2}\right) \end{aligned} \right\} \quad (81)$$

And, for the case where $\{m_j\}_N = \{1\}$ is assumed and N is considerably large, we can apply the following approximations on eqs. (78) ~ (81).

$$\left. \begin{aligned} \frac{\sum_{j=1}^N m_j}{1\tau_N} g &\doteq 191 \left(\frac{2+p}{1+p} \right)^{1/2} (\text{cm/sec}), \left(\frac{\sum_{j=1}^N m_j}{1\tau_N} \right)^2 g \doteq 37.4 \left(\frac{2+p}{1+p} \right) (\text{cm/sec}) \\ \frac{\sum_{j=1}^N p_j}{\sum_{j=1}^N m_j} &\doteq 0.5 \left(\frac{2+p}{1+p} \right), \quad I, (c=1), \end{aligned} \right\} \quad (82)$$

Thus, for the case $N \gg 1$, \bar{V}_{evN} , e_{ev} and p_{ev} are calculated from eqs. (72) and (78) ~ (82) as follows,

the structure B ;

$$\begin{aligned} \bar{V}_{evN} &= 301_1 T \text{ (cm/sec)}, \quad e_{ev} = 46.4_1 T^2 \text{ (cm)}, \quad p_{ev} = 32.5_1 T^2 \text{ (cm)}, \quad 1T < 0.426 \text{ sec} \\ \bar{V}_{evN} &= 128 \text{ (cm/sec)}, \quad e_{ev} = 8.35 \text{ (cm)}, \quad p_{ev} = 5.84 \text{ (cm)}, \quad 0.426 \text{ sec} \leq 1T \leq 2.06 \text{ sec} \\ \bar{V}_{evN} &= 62.1_1 T \text{ (cm/sec)}, \quad e_{ev} = 1.98_1 T^2 \text{ (cm)}, \quad p_{ev} = 1.39_1 T^2 \text{ (cm)}, \quad 2.06 \text{ sec} < 1T \end{aligned}$$

the structure C ;

$$\begin{aligned} \bar{V}_{evN} &= 177_1 T \text{ (cm/sec)}, \quad e_{ev} = p_{ev} = 16.0_1 T^2 \text{ (cm)}, \quad 1T < 0.595 \text{ sec} \\ \bar{V}_{evN} &= 105 \text{ (cm/sec)}, \quad e_{ev} = p_{ev} = 5.61 \text{ (cm)}, \quad 0.595 \text{ sec} \leq 1T \leq 1.68 \text{ sec} \\ \bar{V}_{evN} &= 62.5_1 T \text{ (cm/sec)}, \quad e_{ev} = p_{ev} = 1.98_1 T^2 \text{ (cm)}, \quad 1.68 \text{ sec} < 1T \end{aligned} \quad (83-b)$$

In particular, for the constant maximum velocity characteristics, all of \bar{V}_{ev} , e_{ev} , and p_{ev} are independent on τ_a and $1T$, and also \bar{V}_{evN} and p_{ev} are almost independent on the optimum dynamic characteristics. \bar{V}_{ev} is proportional to the maximum of the maximum velocity amplitudes of the earthquake excitation group as understood from eqs. (49) and (63), and p_{ev} means the

allowable elastoplastic potential energy per unit weight. And so these facts are in accordance with "Velocity-Potential Energy Theory" entitled by Prof. Ryo Tanabashi which states that the violence of earthquakes applied on building structure is proportional to the square of the maximum velocity of the earthquake motion and the resistance of structure is proportional to the conserved potential energy of its structure.

5.3 From Figs. 28 and 29, the base shear coefficient can be formulated by the following expression corresponding to the two different wave shape functions.

El Centro type wave shape function ;

$$\left. \begin{aligned} s({}_1T, \gamma_a; r) &= k(\gamma_a; r) [1 + p(\gamma_a; r) ({}_1T - e)] {}_1T^{-1} \\ e &= 4 \text{ sec for } B_I, \quad e = 3 \text{ sec for } C_{II} \end{aligned} \right\} \quad (84)$$

Vernon type wave shape function ;

$$\left. \begin{aligned} s({}_1T, \gamma_a; r) &= dk(\gamma_a; r) {}_1T^{-1} \\ \bar{d} &= 0.34 \text{ sec for } B_I, \quad \bar{d} = 0.40 \text{ sec for } C_{II} \end{aligned} \right\} \quad (85)$$

where

$$\left. \begin{aligned} k(\gamma_a; r) &= (1-r) [2\gamma_a - 1 + r(\gamma_a - 1)^2]^{-1/2} \\ p(\gamma_a; r) &= 0.04(\gamma_a - 1) + 0.1r^{1/2} \end{aligned} \right\} \quad (86)$$

These formulas are, at least, valid in the case where $2 \leq \gamma_a \leq 5$, $\{\nu_j\}_N = \{1\}$, $0 \leq r \leq 0.2$, $\{\mu_j\}_N = \{1\}$ and $2 \text{ sec} \leq {}_1T \leq 5 \text{ sec}$. The numerical values of eqs. (84) and (85) are shown in Fig. 38 for the structure C_{II} . Substituting eq. (84) or (85) into eq. (59) and solving it with respect to the fundamental natural period ${}_1T$, then ${}_1T$ can be obtained as follows.

El Centro type wave shape function ;

$$\begin{aligned} {}_1T(\bar{A}_N, \gamma_a, N; r) &= \frac{p(\gamma_a; r) - 1 + \left[(e \cdot p(\gamma_a; r) - 1)^2 + \frac{4p(\gamma_a; r)l(\bar{A}_N, N)}{k(\gamma_a; r)} \right]^{1/2}}{2p(\gamma_a; r)} \\ {}_1T(\bar{A}_N, 1, N; 0) &= \frac{l(\bar{A}_N, N)}{k(1; 0)} \end{aligned} \quad (87)$$

Vernon type wave shape function ;

$${}_1T(\bar{A}_N, \gamma_a, N; r) = \frac{l(\bar{A}_N, N)}{dk(\gamma_a; r)} \quad (88)$$

where $l(\bar{A}_N, N)$ is given by eq. (74-b).

Supposing the structure of C_{II} type with $\{m_j\}_N = \{1\}$ and substituting the right hand side of eq. (75) into eq. (74-b), the fundamental natural period ${}_1T$ is plotted in Fig. 39 in the case $\bar{A}_N = 2 \text{ cm}$. The numerical

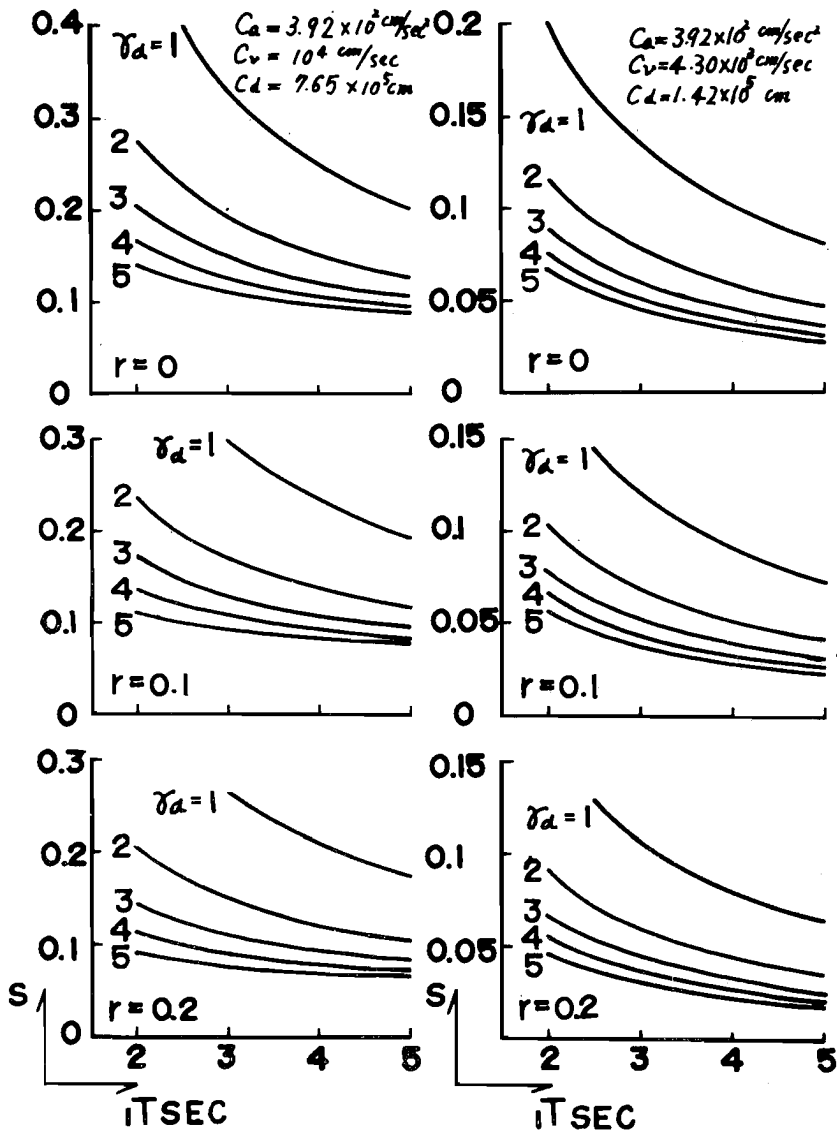
EL CENTRO NS, C_I VERNON S82°E, C_I 

Fig. 38. Base Shear Coefficients for $2 \text{ sec} \leq T \leq 5 \text{ sec}$ —El Centro N-S and Vernon S82°E, Structural Model C_{II} .

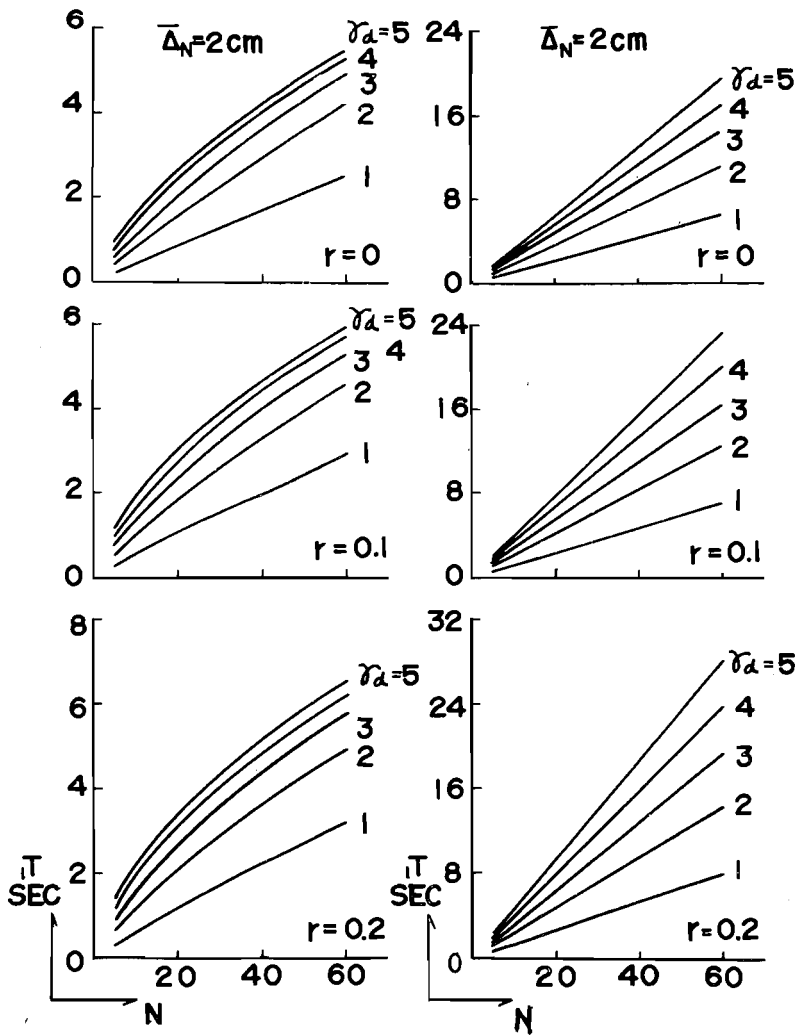
EL CENTRO NS, C_{II} VERNON S82°E, C_{II} 

Fig. 39. Fundamental Natural Period for $\bar{I}_N=2$ cm-El Centro N-S and Vernon S82°E, Structural Model C_{II} .

values of ${}_1T$, for instance, are as follows.

El Centro, C_{II} , $\gamma_a=3$, $r=0.1$;

$$\begin{aligned} N=24 ; \bar{\Delta}_N=1 \text{ cm} \sim {}_1T=1.59 \text{ sec}, \bar{\Delta}_N=2 \text{ cm} \sim {}_1T=2.74 \text{ sec} \\ \bar{\Delta}_N=4 \text{ cm} \sim {}_1T=4.56 \text{ sec} \end{aligned} \quad (89)$$

$$\begin{aligned} N=60 ; \bar{\Delta}_N=1 \text{ cm} \sim {}_1T=3.24 \text{ sec}, \bar{\Delta}_N=2 \text{ cm} \sim {}_1T=5.31 \text{ sec} \\ \bar{\Delta}_N=4 \text{ cm} \sim {}_1T=8.32 \text{ sec} \end{aligned}$$

Substituting eq. (87) or (88) into eq. (84) or (85) respectively, then the base shear coefficients can be obtained as the functions of $\bar{\Delta}_N$, γ_a , N , r , $\{m_j\}_N$ and $\{\kappa_j\}_N$, namely

El Centro type wave shape function ;

$$\begin{aligned} s(\bar{\Delta}_N, \gamma_a, N ; r) = k(\gamma_a ; r) [1 + p(\gamma_a ; r)] \\ \times \left[1 - \frac{2e \cdot p(\gamma_a ; r)}{e \cdot p(\gamma_a ; r) - 1 + \left[(e \cdot p(\gamma_a ; r) - 1)^2 + \frac{4p(\gamma_a ; r)l(\bar{\Delta}_N, N)}{k(\gamma_a ; r)} \right]^{1/2}} \right] \end{aligned} \quad (90-a)$$

$$s(\bar{\Delta}_N, 1, N ; 0) = \frac{1}{l(\bar{\Delta}_N, N)} \quad (90-b)$$

Vernon type wave shape function ;

$$s(\bar{\Delta}_N, \gamma_a, N ; r) = \frac{d^2 k(\gamma_a ; r)^2}{l(\bar{\Delta}_N, N)} \quad (91)$$

On the other hand, the standard values of the equivalent relative velocities \bar{V}_{evN} defined by eq. (63) are obtained by

El Centro type wave shape function ;

$$\bar{V}_{evN} = \bar{V}_{evN}({}_1T, \gamma_a ; r) = (1-r) [1 + p(\gamma_a ; r) ({}_1T - e)] g \frac{\sum_{j=1}^N m_j}{{}_1\tau_N} \quad (92)$$

Vernon type wave shape function ;

$$\bar{V}_{evN} = \bar{V}_{evN}(r) = d(1-r) g \frac{\sum_{j=1}^N m_j}{{}_1\tau_N} \quad (93)$$

And also, e_{ev} and p_{ev} can be determined by the following equations.

El Centro type wave shape function ;

$$e_{ev} = e_{ev}({}_1T, \gamma_a ; r) = \frac{(1-r)^2}{2} [1 + p(\gamma_a ; r) ({}_1T - e)]^2 g \left(\frac{\sum_{j=1}^N m_j}{{}_1\tau_N} \right)^2 \quad (94)$$

Vernon type wave shape function ;

$$e_{ev} = e_{ev}(r) = \frac{d^2(1-r)^2}{2} \cdot g \left(\frac{\sum_{j=1}^N m_j}{{}_1\tau_N} \right)^2 \quad (95)$$

and

$$\dot{p}_{ep} = \frac{\sum_{j=1}^N \dot{p}_j}{\sum_{j=1}^N m_j} \cdot e_{ep} \quad (96)$$

In the case $\{m_j\}_N = \{1\}$, the coefficient $\frac{\sum_{j=1}^N \dot{p}_j}{\sum_{j=1}^N m_j}$ has a same expression as eq. (81) as $\{\nu_j\}_N = \{1\}$ and $\{\mu_j\}_N = \{1\}$ are assumed. Using eqs. (81), (82) and (84)~(86), then the numerical values of \bar{V}_{epN} , e_{ep} and \dot{p}_{ep} are calculated from eqs. (92)~(95) in the case $\{m_j\}_N = \{1\}$, $\{\nu_j\}_N = \{1\}$, $\{\mu_j\}_N = \{1\}$ and $N \gg 1$. Table 1 shows the numerical values at the boundary points in the domain considered here; $2 \leq \gamma_a \leq 5$, $0 \leq r \leq 0.2$ and $2 \text{ sec} \leq {}_1T \leq 5 \text{ sec}$, together with the extrapolated values for the elastic case; $\gamma_a = 1$, $r = 1$.

Table 1. Standard value of equivalent relative velocity for allowable elasto-plastic potential energy, allowable elasto-plastic potential energy factor and total allowable elasto-plastic potential energy coefficient.

El Centro	\bar{V}_{ep} (cm/sec)		e_{ep} (cm)		\dot{p}_{ep} (cm)	
	${}_1T = 2 \sim 5 \text{ sec}$		${}_1T = 2 \sim 5 \text{ sec}$		${}_1T = 2 \sim 5 \text{ sec}$	
$\gamma_a = 1$ $r = 0$	$\left\{ \begin{array}{l} B_I \\ C_{II} \end{array} \right.$	B_I	226~226	26.2~26.2	18.3~18.3	18.3~18.3
		C_{II}	214~214	23.4~23.4	23.4~23.4	23.4~23.4
$\gamma_a = 2$ $r = 0$	$\left\{ \begin{array}{l} B_I \\ C_{II} \end{array} \right.$	B_I	208~235	22.2~28.3	15.6~19.8	15.6~19.8
		C_{II}	206~231	21.6~27.3	21.6~27.3	21.6~27.3
$\gamma_a = 5$ $r = 0.2$	$\left\{ \begin{array}{l} B_I \\ C_{II} \end{array} \right.$	B_I	107~219	5.84~24.5	4.08~17.2	4.08~17.2
		C_{II}	135~241	9.33~29.8	9.33~29.8	9.33~29.8
Vernon	\bar{V}_{ep} (cm/sec)		e_{ep} (cm)		\dot{p}_{ep} (cm)	
	${}_1T = 2 \sim 5 \text{ sec}$		${}_1T = 2 \sim 5 \text{ sec}$		${}_1T = 2 \sim 5 \text{ sec}$	
$\gamma_a = 1 \sim 5$ $r = 0$	$\left\{ \begin{array}{l} B_I \\ C_{II} \end{array} \right.$	B_I	76.8~76.8	3.05~3.05	2.14~2.14	2.14~2.14
		C_{II}	85.6~85.6	3.74~3.74	3.74~3.74	3.74~3.74
$\gamma_a = 1 \sim 5$ $r = 0.2$	$\left\{ \begin{array}{l} B_I \\ C_{II} \end{array} \right.$	B_I	61.5~61.5	1.95~1.95	1.36~1.36	1.36~1.36
		C_{II}	68.5~68.5	2.40~2.40	2.40~2.40	2.40~2.40

On the other hand, \bar{V}_{epN} , e_{ep} and \dot{p}_{ep} are calculated from the third equations of (83-a) and (83-b) as shown in Table 2.

According to these tables, it is found that \dot{p}_{ep} is influenced by the type of structures, but \bar{V}_{ep} and e_{ep} are hardly dependent on the type of them in the case $2 \text{ sec} \leq {}_1T$, and that, for the El Centro type wave shape

Table 2. Standard value of equivalent relative velocity for allowable elasto-plastic potential energy, allowable elasto-plastic potential energy factor and total allowable elasto-plastic potential energy coefficient.

El Centro	\bar{V}_{ep} (cm/sec)	e_{ep} (cm)	p_{ep} (cm)	
	${}_1T=2\sim 5$ sec	${}_1T=2\sim 5$ sec	${}_1T=2\sim 5$ sec	
$\gamma_a=1\sim 7$	$\left\{ \begin{array}{l} B_I \\ C_{II} \end{array} \right.$	124~311	7.92~49.5	5.56~34.8
$\gamma=0$		125~312	7.92~49.5	7.92~49.5

function, \bar{V}_{ep} and e_{ep} are the weak function of ${}_1T$ when both γ_a and γ are small, but they are expressed by the increasing functions of ${}_1T$ when either γ_a or γ is large. This corresponds to the fact that the base shear coefficient is a decreasing function of ${}_1T$ when both γ_a and γ is small, but it is the weak function of ${}_1T$ when either γ_a or γ is large. On the other hand, \bar{V}_{ep} , e_{ep} and p_{ep} are independent on ${}_1T$ in the range $2 \text{ sec} \leq {}_1T \leq 5 \text{ sec}$, in the case of the Vernon type wave shape function. And also, it is considered that the structure of B_I type has the more suitable dynamic characteristics in comparison with that of the structure of C_{II} type in the case $2 \text{ sec} \leq {}_1T \leq 5 \text{ sec}$, particularly when either γ_a or γ is large.

6. Concluding remarks

As regards the ultimate elasto-plastic aseismic design method, the aseismic design data for the initial structural design of the ductile building structures have been obtained by means of the elasto-plastic response analyses. Their design data are induced from the optimum dynamic characteristics which control the aseismic safety of a structure to be uniform within the prescribed allowable value. The wave shape function of earthquake excitations is found to have little effect on the qualitative characteristics of earthquake responses of a structure but considerable effect on the quantitative characteristics of them. For instance, the El Centro type wave shape function is almost identical with the Vernon type function with the intensity two or three times as much as that of the El Centro type. And it is very important that the slightly positive rigidity ratios of bi-linear hysteretic characteristics make the earthquake response remarkably stable and restrain their dispersion considerably in the wide ranges of various parameters. And so it is found that the distributions

of optimum dynamic characteristics have a great significance to obtain the reasonable aseismic design, and that assigning the slightly positive rigidity ratios to a structural system by use of the aseismic structural elements may be very effective. But the standard values of the optimum dynamic characteristics are largely affected by the wave shape function and the frequency characteristics of the maximum amplitude both of which define an excitation group. Therefore, it will be very important to prescribe them reasonable corresponding to the intensity of the group of earthquake excitation and other various conditions. But there are still so many problems to be reexamined in this procedure. And even in the earthquake response analyses, the basic problems concerning the pattern of earthquake excitations, the model of structural system and the measures of aseismic safety should be still more reexamined in the future. Although the effect of ground may be roughly estimated by adjusting the frequency characteristics of the maximum amplitude of ground acceleration, it should be essentially studied on the problem of ground-structure coupling together with the problem of earthquake excitation pattern.

Acknowledgments

The authors wish to express their appreciation to Professor Ryo Tanabashi for his approval in the preparation of this paper. Thanks are also expressed to Mr. Y. Inoue, Mr. K. Tagawa and others for their helpful assistance in carrying out the numerical analyses, and also to the Kyoto University Computer Center for the use of the Digital Computer KDC-I.

Bibliography

- 1) Tanabashi, R. ; On the Resistance of Structures to Earthquake Shocks, Mem. of the College of Engrg, Kyoto Univ., Vol. IX, NO. 4, 1937, pp. 191-205.
- 2) Tanabashi, R., Kobori, T. and Minai, R. ; Aseismic Design and Earthquake Response of Structure, Annuals of Disaster Prevention Research Institute of Kyoto Univ., No. 5, B, March, 1962, pp. 1-32.
- 3) Kobori, T. ; Dynamic Design of Superstructures, Proc. of Japan National Symposium on Earthquake Engineering, Nov., 1962, pp. 305-310.
- 4) Housner, G. W., ; Behavior of Structures During Earthquakes, Proc. of ASCE, Vol. 4, Oct., 1959, pp. 109-129.
- 5) Kobori, T. and Minai, R. ; Elasto-Plastic Response and Aseismic Design of Skyscraper, Annuals of Disaster Prevention Research Institute of Kyoto Univ., No. 6, July, 1963, pp. 44-62.

- 6) Kobori, T. and Minai, R. ; Earthquake Response Analysis and Aseismic Design, Proc. of the 1st Chilean Sessions on Seismology and Earthquake Engineering, July, 1963, pp. 1-17.
- 7) Tanabashi, R., Kobori, T., Kaneta, K. and Minai, R. ; Statistical Properties of Earthquake Accelerograms and Equivalent Earthquake Excitation Pattern, Proc. of the 1st Chilean Sessions on Seismology and Earthquake Engineering, July, 1963, pp. 1-19.
- 8) Tanabashi, R., Kobori, T., Kaneta, K., Minai, R. and Inoue, Y. ; Effect of Foundation Compliance on Earthquake Response of Multistory Building-Along Computer Analysis of Nonlinear Transient Vibration of Structure, No. 6, Trans. of A. I. J., No. 75, August, 1962, pp. 7-12.
- 9) Veletsos, A. S. and Newmark, N. M. ; Effect of Inelastic Behavior on the Response of Simple Systems to Earthquake Motions, Proc. of the 2nd WCEE, 1960, pp. 895-912.
- 10) Kobori, T., Minai, R. and Tagawa, K. ; Elasto-Plastic Response of Multistory Structure Subjected to Strong Motion Earthquake, Proc. of Japan National Symposium on Earthquake Engineering, Nov., 1962, pp. 165-170.
- 11) Bycroft, G. N. ; Yield Displacements in Multistory Aseismic Design, Bull. of SSA, Vol. 50, No. 3, July, 1960, pp. 441-453.
- 12) Penzien, J. ; Elasto-Plastic Response of Idealized Multi-story Structures Subjected to a Strong Motion Earthquake, Proc. of the 2nd WCEE, 1960, pp. 739-760.
- 13) Berg, G. V. and Thomaidis, S. S. ; Energy Consumption by Structures in Strong-Motion Earthquakes, Proc. of the 2nd WCEE, 1960, pp. 681-697.
- 14) Winder, R. W. and Wheeler, W. T. ; Building Code Provisions for Aseismic Design, Proc. of the 2nd WCEE, 1960, pp. 1843-1876.

Publications of the Disaster Prevention Research

Institute

The Disaster Prevention Research Institute publishes reports of the research results in the form of bulletins. Publications not out of print may be obtained free of charge upon request to the Director, Disaster Prevention Research Institute, Kyoto University, Kyoto, Japan.

Bulletins :

- No. 1 On the Propagation of Flood Waves by Shoitiro Hayami, 1951.
- No. 2 On the Effect of Sand Storm in Controlling the Mouth of the Kiku River by Tojiro Ishihara and Yuichi Iwagaki, 1952.
- No. 3 Observation of Tidal Strain of the Earth (Part I) by Kenzo Sassa, Izuo Ozawa and Soji Yoshikawa. And Observation of Tidal Strain of the Earth by the Extensometer (Part II) by Izuo Ozawa, 1952.
- No. 4 Earthquake Damages and Elastic Properties of the Ground by Ryo Tanabashi and Hatsuo Ishizaki, 1953.
- No. 5 Some Studies on Beach Erosions by Shoitiro Hayami, Tojiro Ishihara and Yuichi Iwagaki, 1953.
- No. 6 Study on Some Phenomena Foretelling the Occurrence of Destructive Earthquakes by Eiichi Nishimura, 1953.
- No. 7 Vibration Problems of Skyscraper. Destructive Element of Seismic Waves for Structures by Ryo Tanabashi, Takuzi Kobori and Kiyoshi Kaneta, 1954.
- No. 8 Studies on the Failure and the Settlement of Foundations by Sakurō Murayama, 1954.
- No. 9 Experimental Studies on Meteorological Tsunamis Traveling up the Rivers and Canals in Osaka City by Shoitiro Hayami, Katsumasa Yano, Shohei Adachi and Hideaki Kunishi, 1955.
- No.10 Fundamental Studies on the Runoff Analysis by Characteristics by Yuichi Iwagaki, 1955.
- No.11 Fundamental Considerations on the Earthquake Resistant Properties of the Earth Dam by Motohiro Hatanaka, 1955.
- No.12 The Effect of the Moisture Content on the Strength of an Alluvial Clay by Sakurō Murayama, Kōichi Akai and Tōru Shibata, 1955.
- No.13 On Phenomena Forerunning Earthquakes by Kenzo Sassa and Eiichi Nishimura, 1956.
- No.14 A Theoretical Study on Differential Settlements of Structures by Yoshitsura Yokoo and Kunio Yamagata, 1956.
- No.15 Study on Elastic Strain of the Ground in Earth Tides by Izuo Ozawa, 1957.
- No.16 Consideration on the Mechanism of Structural Cracking of Reinforced Concrete Buildings Due to Concrete Shrinkage by Yoshitsura Yokoo and S. Tsunoda, 1957.
- No.17 On the Stress Analysis and the Stability Computation of Earth Embankments by Kōichi Akai, 1957.
- No.18 On the Numerical Solutions of Harmonic, Biharmonic and Similar Equations by the Difference Method Not through Successive Approximations by Hatsuo Ishizaki, 1957.

- No.19 On the Application of the Unit Hydrograph Method to Runoff Analysis for Rivers in Japan by Tojiro Ishihara and Akiharu Kanamaru, 1958.
- No.20 Analysis of Statically Indeterminate Structures in the Ultimate State by Ryo Tanabashi, 1958.
- No.21 The Propagation of Waves near Explosion and Fracture of Rock (I) by Soji Yoshikawa, 1958.
- No.22 On the Second Volcanic Micro-Tremor at the Volcano Aso by Michiyasu Shima, 1958.
- No.23 On the Observation of the Crustal Deformation and Meteorological Effect on It at Ide Observatory and On the Crustal Deformation Due to Full Water and Accumulating Sand in the Sabo-Dam by Michio Takada, 1958.
- No.24 On the Character of Seepage Water and Their Effect on the Stability of Earth Embankments by Kōichi Akai, 1958.
- No.25 On the Thermoelasticity in the Semi-infinite Elastic Solid by Michiyasu Shima, 1958.
- No.26 On the Rheological Characters of Clay (Part 1) by Sakurō Murayama and Tōru Shibata, 1958.
- No.27 On the Observing Instruments and Tele-metrical Devices of Extensometers and Tiltmeters at Ide Observatory and On the Crustal Strain Accompanied by a Great Earthquake by Michio Takada, 1959.
- No.28 On the Sensitivity of Clay by Shinichi Yamaguchi, 1959.
- No.29 An Analysis of the Stable Cross Section of a Stream Channel by Yuichi Iwagaki and Yoshito Tsuchiya, 1959.
- No.30 Variations of Wind Pressure against Structures in the Event of Typhoons by Hatsuo Ishizaki, 1959.
- No.31 On the Possibility of the Metallic Transition of MgO Crystal at the Boundary of the Earth's Core by Tatsuhiko Wada, 1960.
- No.32 Variation of the Elastic Wave Velocities of Rocks in the Process of Deformation and Fracture under High Pressure by Shogo Matsushima, 1960.
- No.33 Basic Studies on Hydraulic Performances of Overflow Spillways and Diversion Weirs by Tojiro Ishihara, Yoshiaki Iwasa and Kazune Ihda, 1960.
- No.34 Volcanic Micro-tremors at the Volcano Aso by Michiyasu Shima, 1960.
- No.35 On the Safety of Structures Against Earthquakes by Ryo Tanabashi, 1960.
- No.36 On the Flow and Fracture of Igneous Rocks and On the Deformation and Fracture of Granite under High Confining Pressure by Shogo Matsushima, 1960.
- No.37 On the physical properties within the B-layer deduced from olivine-model and on the possibility of polymorphic transition from olivine to spinel at the 20° Discontinuity by Tatsuhiko Wada, 1960.
- No.38 On Origins of the Region C and the Core of the Earth —Ionic-Intermetallic-Metallic Transition Hypothesis— by Tatsuhiko Wada, 1960.
- No.39 Crustal Structure in Wakayama District as Deduced from Local and Near Earthquake Observations by Takeshi Mikumo, 1960.
- No.40 Earthquake Resistance of Traditional Japanese Wooden Structures by Ryo Tanabashi, 1960.
- No.41 Analysis With an Application to Aseismic Design of Bridge Piers by Hisao Goto and Kiyoshi Kaneta, 1960.
- No.42 Tilting Motion of the Ground as Related to the Volcanic Activity of Mt. Aso and Micro-Process of the Tilting Motion of Ground and Structure by Yoshiro Itō 1961.
- No.43 On the Strength Distribution of the Earth's Crust and the Upper Mantle, and

- the Distribution of the Great Earthquakes with Depth by Shogo Matsushima, 1961
- No.44 Observational Study on Microseisms (Part 1) by Kennosuke Okano, 1961.
- No.45 On the Diffraction of Elastic Plane Pulses by the Crack of a Half Plane by Michiyasu Shima, 1961.
- No.46 On the Observations of the Earth Tide by Means of Extensometers in Horizontal Components by Izuo Ozawa, 1961.
- No.47 Observational Study on Microseisms (Part 2) by Kennosuke Okano, 1961.
- No.48 On the Crustal Movement Accompanying with the Recent Activity on the Volcano Sakurajima (Part 1) by Keizo Yoshikawa, 1961.
- No.49 The Ground Motion Near Explosion by Soji Yoshikawa, 1961.
- No.50 On the Crustal Movement Accompanying with the Recent Activity of the Volcano Sakurajima (Part 2) by Keizo Yoshikawa, 1961.
- No.51 Study on Geomagnetic Variation of Telluric Origin Part 1 by Junichiro Miyakoshi, 1962.
- No.52 Considerations on the Vibrational Behaviors of Earth Dams by Hatsuo Ishizaki and Naotaka Hatakeyama, 1962.
- No.53 Some Problems on Time Change of Gravity (Parts 1 and 2) by Ichiro Nakagawa, 1962.
- No.54 Nature of the Volcanic Micro-Tremors at the Volcano Aso, Part 1. Observation of a New Type of Long-Period Micro-Tremors by Long-Period Seismograph by Kosuke Kamo, 1962.
- No.55 Nature of the Volcanic Micro-Tremors at the Volcano Aso, Part 2. Some Natures of the Volcanic Micro-Tremors of the 1st kind at the Volcano Aso by Kosuke Kamo, 1962.
- No.56 Nonlinear Torsional Vibration of Structures due to an Earthquake by Ryo Tanabashi, Takuji Kobori and Kiyoshi Kaneta, 1962.
- No.57 Some Problems on Time Change of Gravity (Parts 3, 4 and 5) by Ichiro Nakagawa, 1962.
- No.58 A Rotational Strain Seismometer by Hikaru Watanabe, 1962.
- No.59 Hydraulic Model Experiment Involving Tidal Motion (Parts 1, 2, 3 and 4) by Haruo Higuchi, 1963.
- No.60 The Effect of Surface Temperature on the Crustal Deformations by Shokichi Nakano, 1963.
- No.61 An Experimental Study on the Generation and Growth of Wind Waves by Hideaki Kunishi, 1963.
- No.62 The Crustal Deformations due to the Source of Crack Type (1) by Shokichi Nakano, 1963.
- No.63 Basic Studies on the Criterion for Scour Resulting from Flows Downstream of an Outlet by Yoshito Tsuchiya, 1963.
- No.64 On the Diffraction of Elastic Plane Pulses by a Crack of a Half Plane (Three Dimensional Problem) by Michiyasu Shima, 1963.
- No.65 A Study on Runoff Pattern and its Characteristics by Tōjiro Ishihara and Takuma Takasao, 1963.
- No.66 Application of Extreme Value Distribution in Hydrologic Frequency Analysis by Mutsumi Kadoya, 1964.
- No.67 Investigation on the Origin Mechanism of Earthquakes by the Fourier Analysis of Seismic Body Waves (1) by Yoshimichi Kishimoto, 1964.
- No.68 Aseismic Design Method of Elasto-Plastic Building Structures by Takuji Kobori and Ryoichiro Minai, 1964.

Bulletin No. 68 Published March, 1964

昭和 39 年 3 月 20 日 印 刷

昭和 39 年 3 月 25 日 発 行

編 兼
發 行 者 京 都 大 学 防 災 研 究 所

印 刷 者 山 代 多 三 郎

京都市上京区寺之内通小川西入

印 刷 所 山 代 印 刷 株 式 会 社